E/p Systematics from the W Electron Sample

A. B. Wicklund and K. Byrum

24 May 1993

In this note, we use E/p from the W-electron sample to understand false curvatures in the tracking, both the 6.01 data available for the full inclusive electron sample, and the 6.10 data available for the "full" W electron sample (Stream 2 files 0-56). We compare beam-constrained and SVX-linked tracking, in order to verify that the beam-constraint gives the same E/p resolution as the SVX fit, and so allows for good-quality momentum reconstruction for both SVX and non-SVX tracks, using the same (CTC + beam constraint) tracking. Although 6.01 tracking is "obsolete", we are using it for the 9 GeV inclusive electron sample to get E/p tower corrections and to do B physics. Thus, it is generally useful to be able to "improve" 6.01 tracking so that it is demonstrably as good as 6.10.

1) Selection

The W-electron selection follows that described in an earlier note, in which we compared 1989 and 1992 calorimeter response. The basic cuts are:

- Abs (zvertex) < 60
- Abs (Z0-zvertex) < 6 cm.
- Etmiss > 20 (uncorrected)
- Abs(Xlocal) < 21.5
- 10 < Zlocal < 205 cm
- Et > 25 GeV
- Lshr (3T) < 0.2
- Had/Em (3T) < 0.04
- Eborder < 2 GeV
- N(3D) = 1 in 3-tower cell
- Abs (ϕ (electron) - ϕ (neutrino)) in [$\pi/2$, 3 $\pi/2$]
- Abs (DVX_{ctc}) < 0.3 cm

In addition we differentiate "good" electrons in the above sample by the strip-chamber cuts:

- Abs (dX) < 1 cm.
- Abs (dZ) < 3 cm
- $\chi^2_x < 10$
- $\chi^2_z < 10$

The latter cuts are biased against Brehm's, as well as any non-electron backgrounds. Figure 1 shows the E/p distributions for "good electrons" (shaded), and electrons that fail the above CES cuts (solid points, scaled X 10). For all alignment studies below we make the CES cuts to avoid brehm smearing. We note that the good electron fraction is about the same for SVX-linked tracks as for non-SVX tracks. The fractions failing the CES cuts are:

- 13.5 ± 0.9% (1382 non-SVX electrons)
- 13.3 ± 0.6% (3482 SVX electrons)

This suggests that the equivalent radiators are similar for the two samples, though we might have expected more radiator and more failures for the SVX tracks.

2) <u>Determination of Beam Spot</u>

We have obtained the SVX beam spots from the data base, thanks to Hans Wenzel and John Skarha. To check these beam spots, we obtained (X0,Y0) for each run using the inclusive electron (6.01 tracking) sample; we used only tracks above 1 GeV/c, in a cone of radius 1.2 around the electron. Our (X0,Y0) are plotted versus run number in Fig. 2 (crosses), together with the data base beam spots to run 43000 (histogram). They agree within 10 μM or so. The (X0,Y0) points are evaluated at Z = 0; we binned the tracks in Zvertex, and plotted the differences, (X(Z) - X(0)), (Y(Z) - Y(0)), in Fig. 3. They follow a straight line in Z, consistent with the results obtained by Hans Wenzel (CDF-1924). We also plot the differences between the CTC beam spot and the SVX beam spot, obtained from tracks in the electron sample that have both CTC and SVX fits. These differences are also plotted in Fig. 3 (crosses = dX, circles = dY), where each view is defined by, e.g.,

$$dX = [X(Z) - X(0)]\ ctc - [X(Z) - X(0)]\ svx.$$

We conclude that, perhaps fortuitously, the Z dependence of the beam spot is the same for CTC and SVX. The actual slopes for the SVX beam spot are plotted in Fig. 4, (crosses), together with the database slopes (histogram), as functions of run number. On average, we have dX0/dZ = + 4 μM/cm, and dZ0/dZ = - 3 μM/cm. Finally, Fig. 5 shows the difference between CTC and SVX beam spots, that is, dX (z = 0) and dZ (z = 0), versus run number. The CTC beam spots themselves are of

course poorly determined compared with the SVX beam spots, but we see that on average,

- dX (CTC - SVX) = 0
- dY (CTC - SVX) = + 80 μM

If the CTC and SVX alignment parameters are independent of run number, then we would expect the offsets between CTC and SVX, both X0,Y0, and dX0/dZ, dY0/dZ, to be constants independent of run, and that would be consistent with the data. We will henceforth assume that this is the case.

3) Systematic Offsets Observed for dvx

We next examine the W electron sample for systematic alignment offsets between CTC and SVX fits. We perform a parallel analysis on both 6.10 and 6.01 W electrons. Figure 6 shows the impact parameter distribution for good W electrons using the SVX track fit, relative to the SVX beam spot. For high Pt tracks that intersect the beam spot at (X0, Y0), the expected dvx is given by the equation:

$$dvx(\phi) = -X0 \sin(\phi) + Y0 \cos(\phi). \qquad (1)$$

Here (X0, Y0) are taken from the SVX beam spot data described above. In Fig. 6, we form the difference,

$$dvx\,(\text{measured}) - dvx\,(\phi)$$

to define the impact parameter relative to the beam spot. To avoid possible confusion, we have attempted to spell out the definition of "dvx" in Appendix I. Figure 6 compares V6.10 and V6.01 tracks, using the same (X0, Y0) values for both. Except for a tail in the 6.10 sample (which we attribute to missing database X0, Y0, where we choose the nearest run number), both versions are quite similar, and exhibit an rms of ± 40 μM, consistent with the assumed beam spot size. We conclude that it is fair to use the same beam spots for both tracking versions, although our direct checks, described in Section (2) above, were for 6.01 tracking only.

Figure 7 shows the dvx versus ϕ plot for good W electrons, using dvx from the CTC, Fig. 7a, and the difference, dvx (SVX) - dvx (CTC), Fig. 7b. Figure 7a just shows that the run-averaged beam spot is at

$$X0 = 600\ \mu M$$
$$Y0 = 0\ \mu M,$$

by comparison of the sinusoid with Eq.(1). This is as expected from the SVX beam spots of Fig. 2. The SVX-CTC difference plot in Fig. 7b is consistent with

$$\text{dvx (SVX) - dvx (CTC)} = -(17 \pm 7) + (80 \pm 10) \sin(\phi - 2.1)\ \mu\text{M} \tag{2}$$

(6.10 tracking)

Physically, if there were no alignment errors, then dvx would follow a perfect sinusoid, with no offset. We remark that dvx (SVX) is indeed a perfect sinusoid, and the 17 μM offset above is due to the behavior of dvx (CTC) only. This 17 μM ϕ-independent offset tells us that the CTC tracks, swum back to the CTC beam spot, point to a circle of radius 17 μM. In addition, the 80 μM sinusoidal variation in the difference tells us that the CTC beam spot is displaced by 80 μM with respect to the SVX beam spot. From the phase of the sinusoid, by comparison with Eq. (1), the displacement is approximately along the Y0 direction, as we anticipated from the discussion in Section (2) (cf, Fig. 5). Figure 8 shows that the difference, dvx (SVX) - dvx (CTC), is the same for e^+ and e^-, within errors. Figures 9 and 10 show the corresponding dvx behavior for 6.01 tracking. The dvx difference here is consistent with:

$$\text{dvx (SVX) - dvx (CTC)} = +(43 \pm 14) + (80 \pm 20) \sin(\phi - 2.1)\ \mu\text{M} \tag{3}$$

(6.01 tracking)

The beam spot displacement of 80 μM is approximately the same for 6.01 and 6.10 tracking, but the ϕ-independent offset has opposite sign in 6.01 (+ 43 versus -17 μM).

We expect false curvatures in the tracking to be correlated with offsets in dvx. The false curvatures are measured by examining the quantity

$$D = E/p\ (e^-) - E/p\ (e^+)$$

Let us first consider the ϕ-averaged false curvature, which we will call "D0", the zeroth harmonic. If D0 is nonzero, due to ϕ-independent rotations of the CTC SL's, then we can expect correlated offsets in dvx, the apparent impact distance between the extrapolated CTC track and the actual (CTC-centered) average beam spot. The tracks will appear to point back, not to the (CTC-centered) beam spot, but to a circle around that beam spot. In particular, we expect

$$\text{dvx (CTC)} = \text{dvx (X0', Y0')} + a0,$$

where X0', Y0' is the CTC beam spot, and where dvx (X0', Y0') is defined by Eq. (1). The offset, a0, will be correlated with the false curvature, "D0", by

$$D0 < 0 \iff a0 > 0.$$
$$D0 > 0 \iff a0 < 0.$$

This can be seen by drawing pictures, see Fig. 11. In the data, before applying any SVX or beam constraint, we observe the following ϕ-averaged offsets:

Vers.	(D0)	(a0)
(6.10)	- .020 ± .003	+ 17 ± 7 μM
(6.01)	+ .011 ± .005	- 43 ± 14 μM

The sign correlation is as expected, and these a0, D0 offsets are simply the zeroth harmonics in the CTC misalignments.

We emphasize that simple CTC misalignments, which shift the helix parameters ("crv", "ϕ", "dvx") systematically, will give the same sign errors in a0 and curvature for both e^+ and e^-. (See Appendix I for explication on helix parameters, especially dvx.) Any mechanism that gives a charge-dependent offset in a0 will be correlated with a charge dependent curvature error, that is, an overall scale error on abs (Pt) for both e^+ and e^-. Brehmsstrahlung is such a mechanism. Referring again to Fig. 11, the effect of external brehms would be to increase the magnitude of the curvature for both e^+ and e^-, and to move the apparent dvx for e^+ and e- to opposite sides of the beam spot at (X0,Y0), e.g. a0 > 0 for e^+, and a0 < 0 for e^-. Such an offset would be manifest in Figs. (8, 10); we would expect the data points for e^+ (e^-) to lie below (above) the (common) solid curve. Perhaps that happens, statistics are marginal.

4) <u>Beam Constraint and First Harmonic Misalignments</u>

We next develop a beam constraint to improve the momentum resolution. Such a constraint is intrinsically ϕ-dependent (unless the beam spot happens to coincide with the origin!), and affects 0'th and 1'st harmonics if there are any ϕ-dependent alignment errors. Any beam constraint, including the SVX track fit, will take the following form:

$$C\ (\text{constrained}) - C\ (\text{measured}) = W * [\text{dvx}\ (\text{meas}) - \text{dvx}\ (X0,Y0)],$$

where C (constrained) and C (measured) are the curvatures after and before the constraint, and W is a weight factor that depends on the error matrices. Any systematic error in the determination of X0, Y0, for example the 80 μM offset between the apparent (X0, Y0) in CTC and SVX, will introduce a correlated sinusoidal error in C (constrained), in addition to any errors that are already present in C (measured).

We digress to specify the precise form of the beam constraint. Rather than compute the quantity "W" from the error matrices, we prefer to determine "W" empirically by optimizing the E/p resolution. This is illustrated in Figs. 12 (6.10

tracking) and 13 (6.01 tracking). We plot the E/p resolution, as a function of the weight parameter; in Figs. 12a and 13a we plot the resolution on E/p for CTC-fitted tracks, and in Figs. 12b and 13b the resolution for SVX fitted tracks, where in both cases we constrain the tracks to the SVX beam spot. The SVX track fits are not significantly improved by this pull, because the SVX tracks already satisfy the beam constraint (dvx (meas) = dvx (X0,Y0)). The CTC fitted tracks show a clear minimum in the resolution with a weight factor of .04; the same result was obtained in the 88-89 data. Figure 14 shows E/p distributions for four different weight factors, for CTC tracks. We define our beam constraint by the equation

$$1/p\ (\text{constrained}) - 1/p\ (\text{measured}) = -\text{weight} \times Q \times [\text{dvx (meas)} - \text{dvx (X0, Y0)}] \tag{4}$$

where Q is the charge and p is absolute transverse momentum.

Thus, if we beam constrain to the SVX beam spot, as is implicitly done in the SVX track fit for example, then we can expect a first harmonic error in E/p correlated with the 80 μM displacement between CTC and SVX beam spots. For the ϕ-averaged misalignments, we observed that a 20 - 40 μM error in dvx (a0 term) corresponds to a .01 - .02 error in the E/p (e^- - e^+) difference, D0. Thus we might expect that the 80 μM beam spot difference would correspond to of order .02 - .04 sinusoidal error on D0. With the precise beam constraint of Eq. (4), with weight = 0.04, we get

$$\delta\,(1/p) = -.04 \times Q \times (-.0080 \sin(\phi - 2.1))$$

or

$$\delta\,(D) = -.022 \sin(\phi - 2.1)$$

for 35 GeV/c tracks.

This is in addition to any first harmonic errors already present in D(ϕ). The main points here are that (1) there is an average 80 μM offset between the CTC and SVX beam spots; (2) when we beam constrain to the SVX beam spot, we will then introduce a first harmonic modulation in E/p; (3) such a modulation is presumably implicit in the SVX fitted tracks.

Figure 15a shows the ϕ dependence of the false curvature, D, for 6.10 CTC tracks. Figure 15b shows the same D versus ϕ, this time after constraining the tracks to the CTC beam spot (not the SVX beam spot). The CTC beam spot is defined by adding the 80 μM modulation to the SVX run-dependent beam spot. The curves are "theory", derived below. The data exhibit sinusoidal and ϕ-averaged offsets in D (and random ones as well). When we constrain to the CTC beam spot, we expect that the beam constrained D will have no additional first harmonic, over and above that already present in the raw CTC fits. That is consistent with Fig. 15. Figure 16 shows the same plots for 6.01 tracking. Here the ϕ-averaged offsets are opposite in sign, and the intrinsic first harmonic is closer to zero.

Next we introduce the SVX beam spot. Figure 15c shows D versus ϕ for SVX-fitted tracks. A clear first harmonic is present, given by the curve

$$D(\phi) = (-.015 \pm .002) - .0625 \sin(\phi - 2.1) \text{ (6.10 tracking)} \tag{5}$$

Figure 15d shows the result of fitting the CTC tracks to the SVX beam spot, using our beam constraint with weight = .04. The curves are the same as for 15c, to facilitate comparison. The curves shown in Figs. 15a, b are obtained by subtracting the contribution of our beam constraint from the fitted curve of 15d. The beam constraint to the SVX vertex introduces an additional first harmonic, which makes the sinusoidal behaviour of Figs. 15c and d more exaggerated than the raw E/p of Fig. 15a. The beam constraint also changes the ϕ averaged value of D0 from D0 = - .020 (raw CTC) to D0 = -.015 (constrained). Finally, Figs. 16c and 16d show the same comparisons for 6.01 tracking. For 6.01 tracking, the SVX track fits give

$$D(\phi) = (-.001 \pm .003) - .0470 \sin(\phi - 2.4) \text{ (6.01 tracking).} \tag{6}$$

Again, the ϕ-averaged offset, -.001, differs from the ϕ-averaged CTC offset (+ .011) simply because of the effect of the beam pull on the ϕ-averaged dvx error. Specifically

$$\begin{aligned} \text{D0 (constrained)} &= \text{D0 (raw CTC)} - 2 \times \text{Et} \times \text{weight} \times \text{a0} \\ &= \text{D0 (raw CTC)} - 2.8 \times \text{a0 (cm)} \end{aligned}$$

The main points here are: (1) within errors, the false curvature, D, has the same 0'th and 1'st harmonics for SVX-fitted tracks and for SVX-beam constrained tracks, using our beam constraint; (2) with no SVX fits, the CTC tracks exhibit nonzero 0'th and 1'st harmonics in D; fitting these to the CTC beam spot preserves the first harmonic, but pulls the 0'th harmonic (i.e. forces tracks to point to the beam spot instead of a circle around the spot). We EMPHASIZE, that fitting the CTC tracks with a beam constraint certainly improves the resolution, but does NOT get rid of the effects of CTC misalignment. Fitting to the actual CTC beam spot can remove only the zeroth harmonic in D, and fitting to the SVX beam spot actually worsens the first harmonic, though of course, that is an unlucky accident having to do with the way the CTC is misaligned and the way the SVX-CTC axes are misaligned.

Clearly it would be desirable to remove all misalignments from CTC tracks, and to eliminate the 80 μM offset between CTC and SVX beam spots. But why bother (80 μM is just barely bigger than the CTC wire diameter!). If we pull CTC tracks to the SVX beam spot, we introduce the same 0'th and 1'st harmonics that are implicit in the SVX fits. So we simply remove the false curvature by hand, using the parametrizations given above for $D(\phi)$. The results are shown in Figs. 17 (6.10 tracking) and 18 (6.01 tracking), for both the SVX track fits (17a, 18a) and the CTC tracks constrained to the SVX vertex (17b, 18b). The curves are the parametrizations of the uncorrected D versus ϕ behavior. Figure 19 shows the com-

parison of E/p distributions for the SVX fitted tracks and the SVX-beam constrained tracks; Fig. 19a shows 6.10 tracking and 19b 6.01 tracking. After correcting the false curvature, the SVX fits and the beam constrained fits give identical resolution. Figure 20 shows a comparison of the corrected E/p for SVX tracks, between 6.01 and 6.10 tracks (normalized to the same number of events). The resolutions are identical. For comparison, Fig. 21 shows the E/p distributions for 6.01 and 6.10 tracking with no SVX fit or SVX beam constraint. Here 6.01 is worse than 6.10 as everyone knows. Figure 22 shows the event-by-event difference between the SVX tracking E/p and the SVX-beam spot constrained CTC tracking. The rms on the difference is 2.7% (3.7%) for 6.10 (6.01) tracking, and the E/p difference is

$$< E/p\,(BC) - E/p\,(SVX) > = 0.0015 \pm 0.0005\ (6.10)$$

This difference is somewhat sensitive to the way we make the false curvature corrections.

For completeness, Figs. 23-26 show the mean values of E/p versus run number for the BC and SVX fits (23, 24) and the rms widths of E/p for the BC and SVX fits (25, 26).

5) Summary

We conclude that, if we apply an explicit false curvature correction to E/p, we can get identical E/p resolution for

- SVX-fitted tracks
- CTC tracks constrained to SVX beam spot
- 6.01 tracking
- 6.10 tracking

Thus, for W physics, it is probably best to use one choice of tracking, namely the beam constraint to the SVX vertex (plus correction), which can be applied uniformly to all electrons independent of Z-vertex or SVX coverage.

APPENDIX I

The CDF definition of dvx and curvature are a potential source of confusion. Here we pause to define dvx more precisely. A fitted helix, with or without SVX hit information, is defined by five parameters which we can take to be "crv, ϕ, dvx, z0, cotθ" in an obvious notation. The half-curvature, "crv" is defined as

$$1/\mathrm{crv} = 2*R\ (\mathrm{cm})$$

$$Pt(\mathrm{GeV/c}) = 0.00299792458 * 1.4116 * R\ (\mathrm{cm})$$

Note that "crv" and Pt are signed by the charge. All quantities are evaluated at the distance of closest approach between the helix and the origin (X,Y = 0,0); thus, while "crv" is constant (except for energy loss) along the helix, "ϕ" increases (decreases) for e^+ (e^-) linearly with path length. The impact parameter is defined as

$$\mathrm{dvx} = -X \sin(\phi) + Y \cos(\phi),$$

where (X, Y) are the coordinates at the distance of closest approach to the origin. This definition is such that dvx is positive for e^+ (e^-) if the origin at (0, 0) lies outside (inside) the helix; dvx is negative for e^+ (e^-) if the origin lies inside (outside) the helix. Now suppose that the track intersects an event vertex or beam spot at the point (X0,Y0). The azimuth at that point on the helix will be different from the parameter "ϕ", which refers to the point (X, Y). A bit of trigenometry reveals the following relationship:

$$\mathrm{dvx} = -X0 \sin(\phi) + Y0 \cos(\phi) - R*[1- \cos(\phi' - \phi)],$$

where dvx and ϕ are the original helix parameters, and ϕ' is the azimuth for the helix at the point (X0,Y0). If (X0,Y0) is close to the origin, that is

$$L = \sqrt{[(X0-X)**2 + (Y0-Y)**2]} << 1\,\mathrm{cm}\ ,$$

then we can expand in ($\phi' - \phi$) and obtain

$$\mathrm{dvx} = -X0 \sin(\phi) + Y0 \cos(\phi) - L *[L/2R]$$

The correction term is very small for the L values that are relevant in CDF, since the beam spots are typically of order 1000 μM from the origin, and R is given by

$$R = Pt(\mathrm{GeV/c}) * 236.30218\ (\mathrm{cm}).$$

For example, for L = 1000 μM and Pt = 35 GeV/c, the above equation reads

$$dvx = - X0 \sin(\phi) + Y0 \cos(\phi) - 0.006\ \mu M$$

The correction term is 1600X smaller than the SVX 10 μM resolution. Thus we can safely ignore the correction term, and write simply

$$dvx(\phi, X0, Y0) = - X0 \sin(\phi) + Y0 \cos(\phi).$$

That is, IF a track intersects the point (X0,Y0), then the fitted parameters dvx and ϕ are related by this equation. Thus it makes sense to look at distributions in the difference, dvx (measured) - dvx (ϕ, X0,Y0), which is, to an excellent approximation, just the distance between the helix and the point (X0,Y0) at the distance of closest approach to (X0,Y0).

APPENDIX II

We summarize the results in terms of a few equations. We use numbers from 6.1 tracking for illustration. First, in the absence of any beam spot or SVX information, we have the systematic errors on the track parameters from residual misalignments of the CTC:

$$dvx\ (CTC) = dvx\ (X0,Y0) + (a + b \sin(\phi - \phi 0) + \text{higher harmonics})$$

$$Q/p\ (CTC) = Q/p\ (true) - (a' + b' \sin(\phi - \phi 1) + \text{higher harmonics}).$$

where

a	=	.0017 cm
b	=	-.0080 cm
a'	=	-.010/35
b'	=	-.020/35 (35= mean Et for W's)

Actually b' is not so well defined -- there appear to be higher harmonics in the raw E/p ($e^- e^+$) difference.

When we apply a beam constraint to the svx spot, we get

$$Q/p\ (BC) = Q/p\ (CTC) - W \times (dvx\ (CTC) - dvx\ (X0,Y0))$$

Combining the misalignments with the beam (or SVX) fit, and using the observed offset between dvx (CTC) and dvx (X0,Y0) = dvx(SVX), we get

$$Q/p\ (BC) = Q/p\ (true) - [(a' + W \times a) + b' \sin(\phi - \phi 1) + W \times b \sin(\phi - \phi 0)]$$

The combined harmonic gives

$$Q/p\ (BC) = Q/p\ (true) - [-.00022 - .00089 \sin(\phi - 2.1)]$$

where we have combined the nominal values listed above and assumed W = .04 in the BC expression. From the fitted E/p difference (Eq.(5) for D), using Et = 35 GeV for the W electrons, we obtain

$$Q/p\ (SVX) = Q/p\ (true) - [-.00021 - .00089 \sin(\phi - 2.1)]$$

The values are consistent, and illustrate the different effects that modulate 1/p. For comparison

a'	=	- .00029
W*a	=	+ .00007
b'	=	- .00057
W*b	=	- .00032

The actual corrections to 1/p are obtained by

1) applying BC to get Q/p (BC), and

2) applying empirical correction to get Q/p (true) from Q/p (BC).

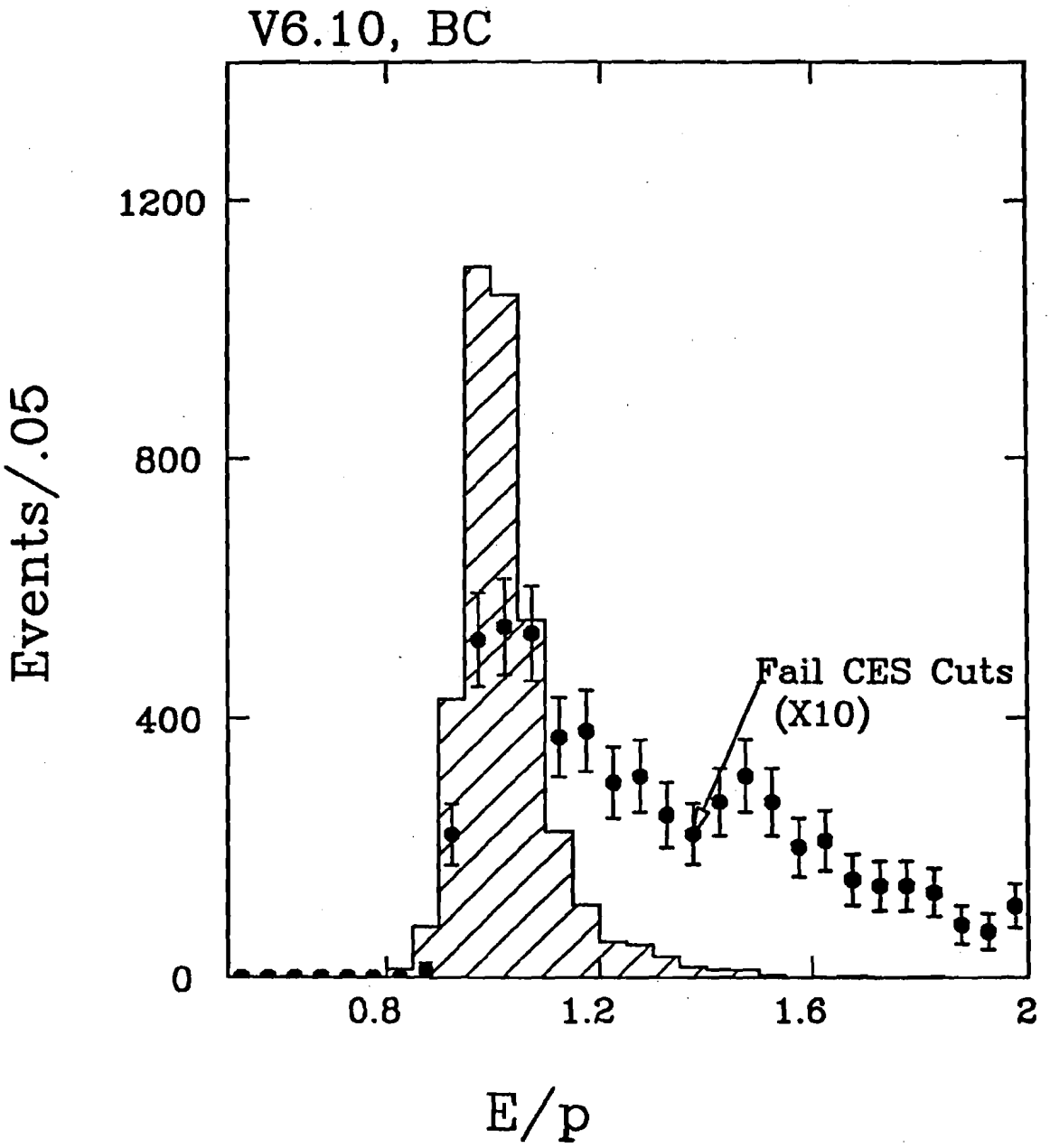

Figure 1

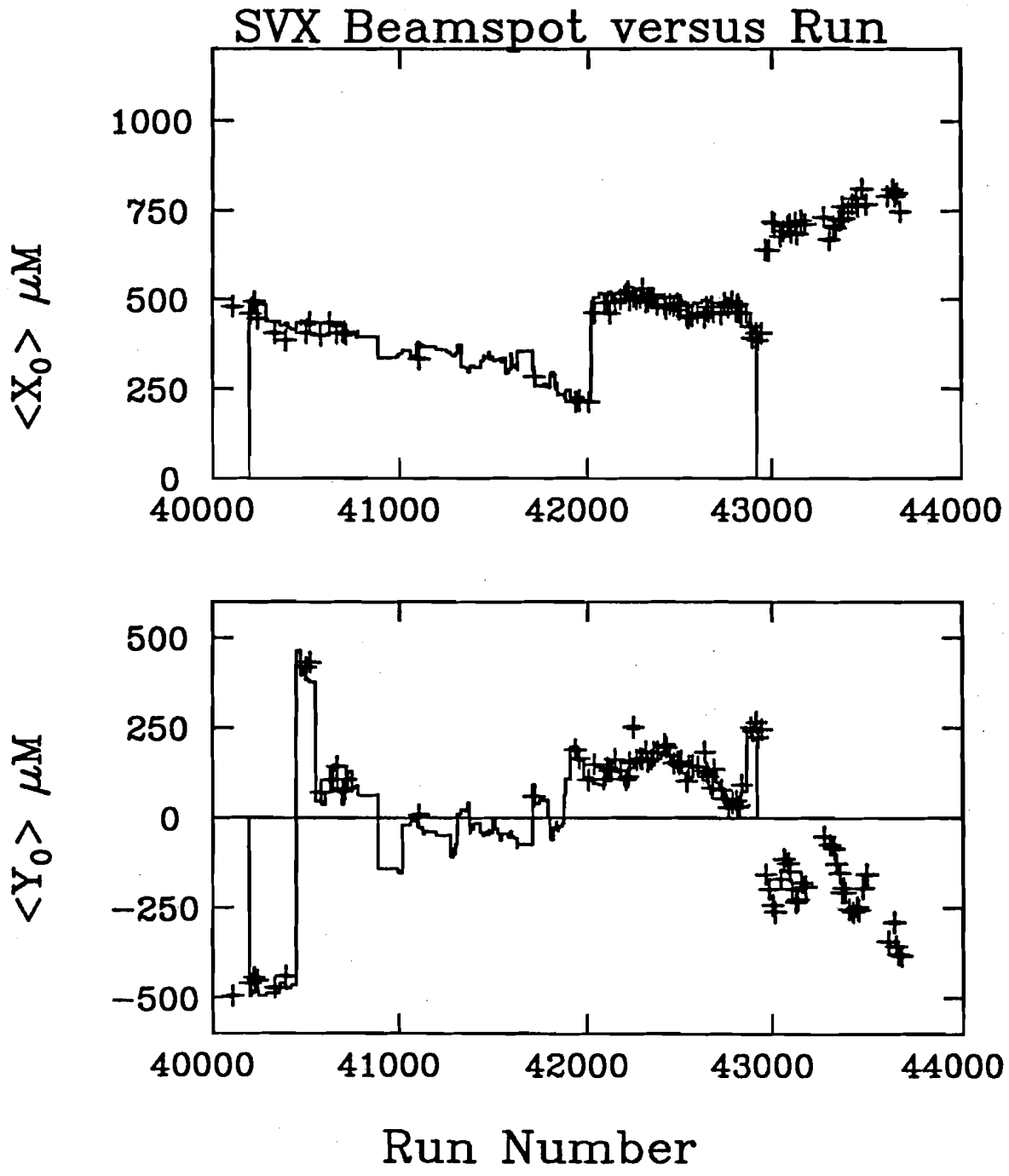
SVX Beamspot versus Run
1000
750
500
250
0
<X0> μM
40000
41000
42000
43000
44000
500
250
0
−250
−500
<Y0> μM
40000
41000
42000
43000
44000
Run Number

Figure 2

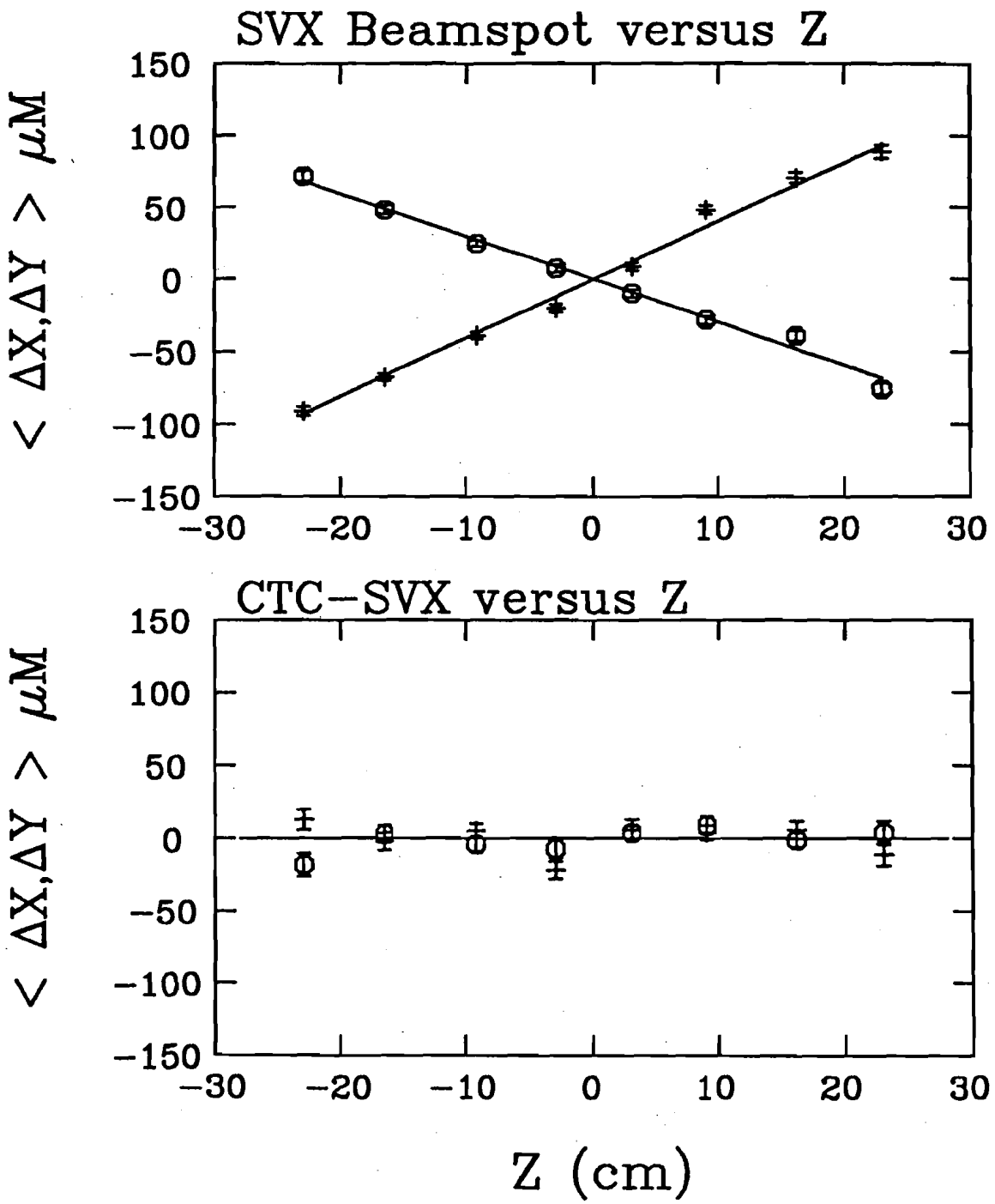
SVX Beamspot versus Z
< ΔX,ΔY > μM
150
100
50
0
−50
−100
−150
−30
−20
−10
0
10
20
30
CTC−SVX versus Z
< ΔX,ΔY > μM
150
100
50
0
−50
−100
−150
−30
−20
−10
0
10
20
30
Z (cm)

Figure 3

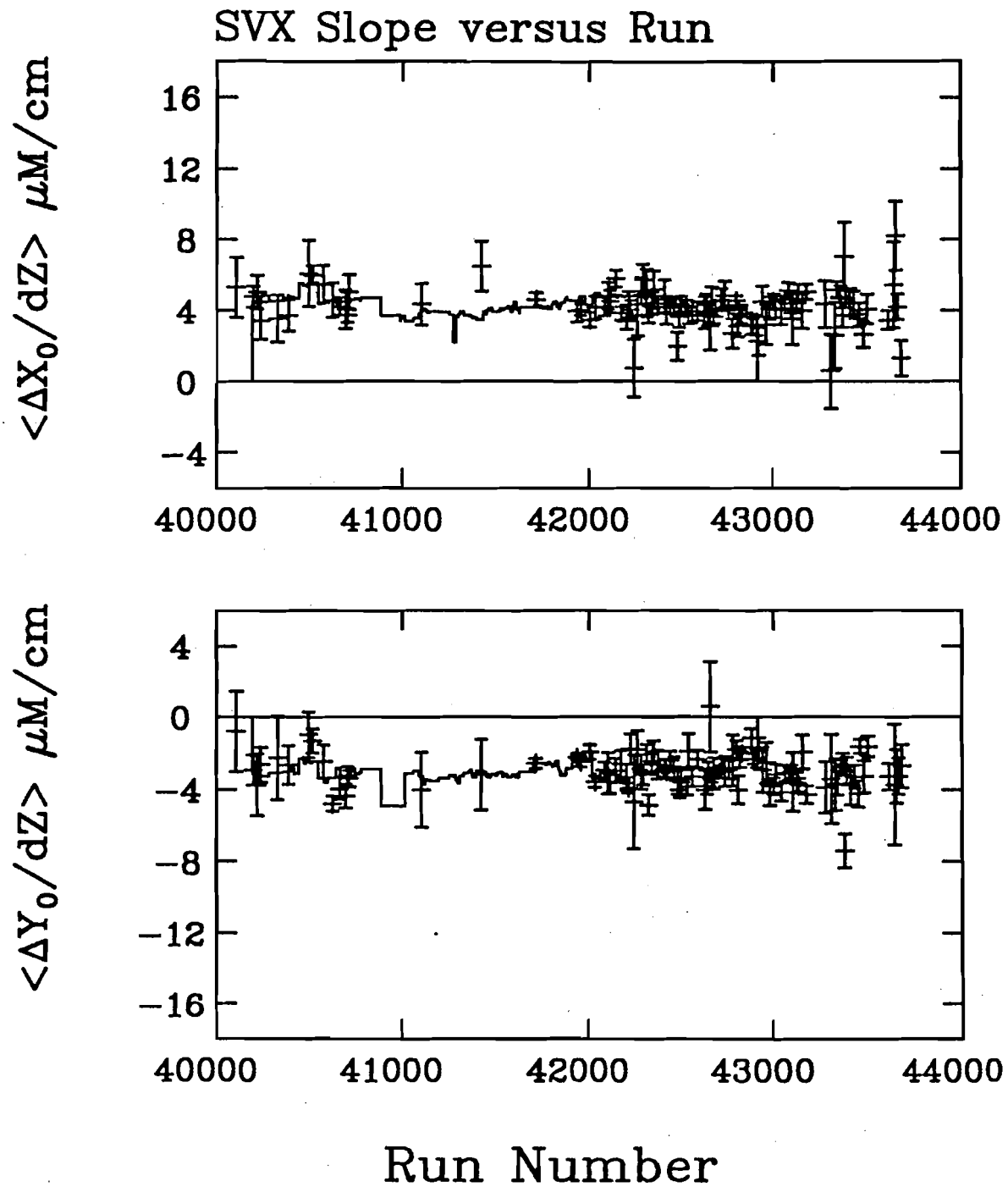
SVX Slope versus Run
<ΔX0/dZ> μM/cm
16
12
8
4
0
−4
40000
41000
42000
43000
44000
<ΔY0/dZ> μM/cm
4
0
−4
−8
−12
−16
40000
41000
42000
43000
44000
Run Number

Figure 4

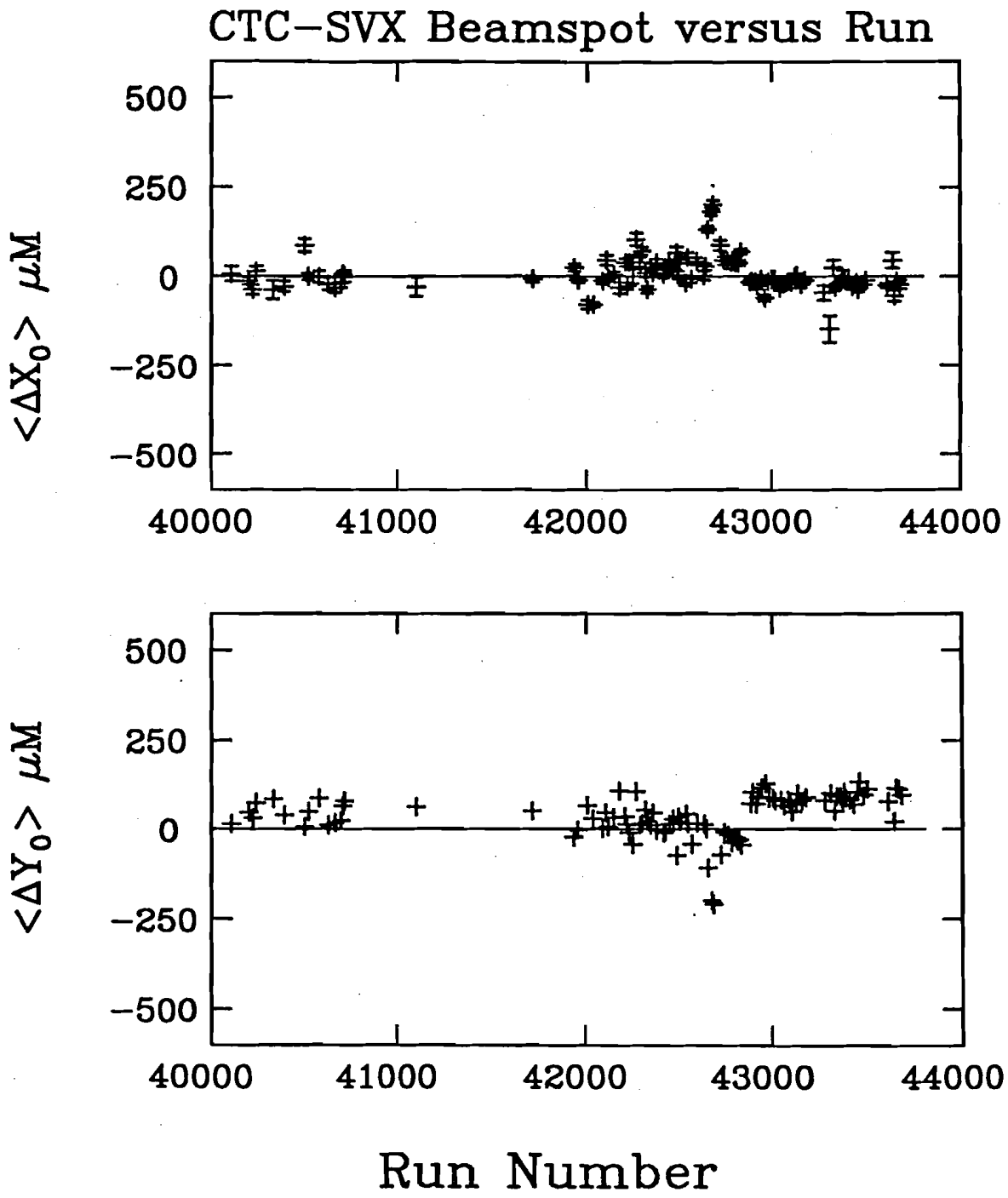
CTC−SVX Beamspot versus Run
500
250
0
−250
−500
<ΔX0> μM
40000
41000
42000
43000
44000
500
250
0
−250
−500
<ΔY0> μM
40000
41000
42000
43000
44000
Run Number

Figure 5

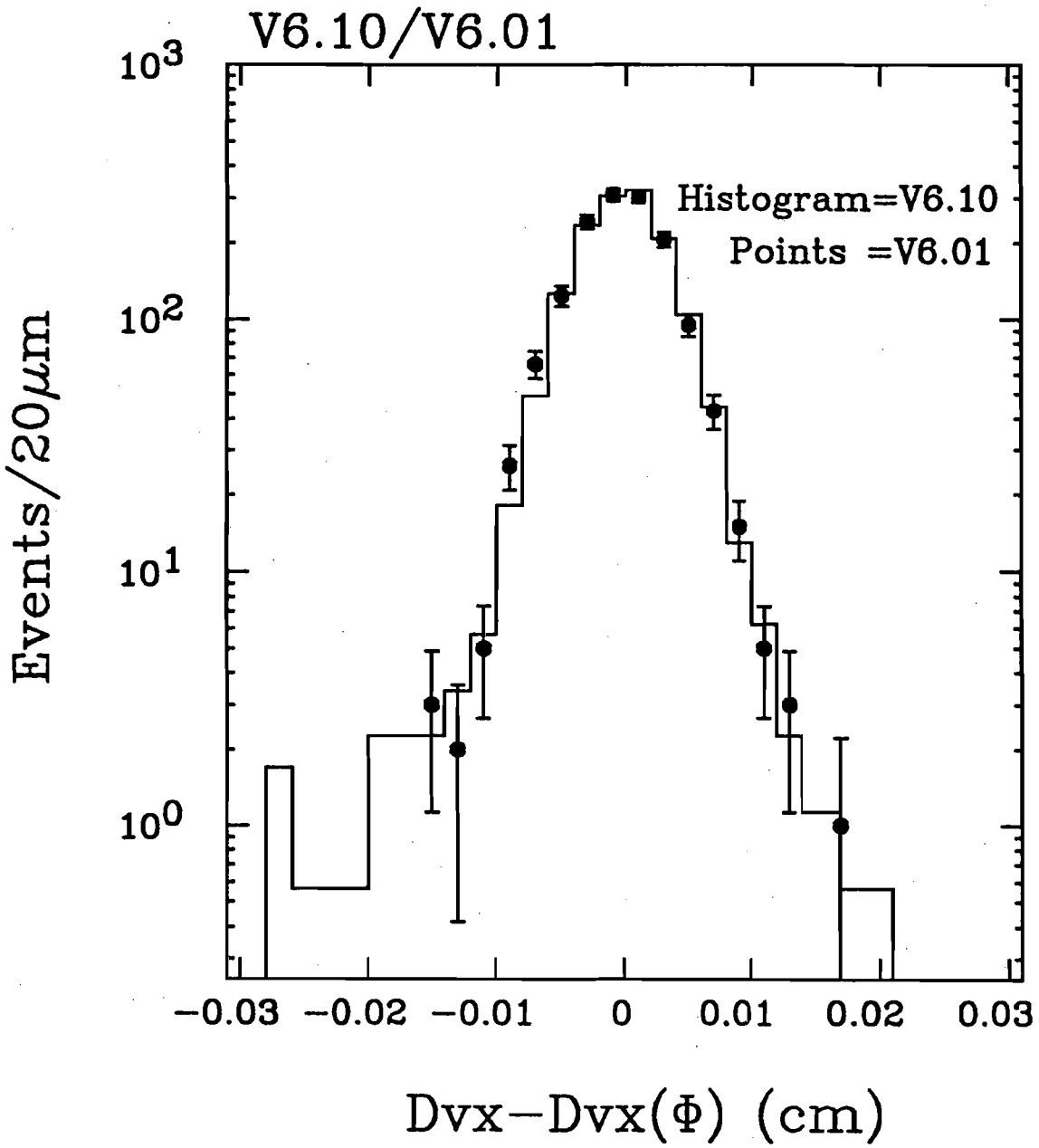
V6.10/V6.01
Histogram=V6.10
Points =V6.01
Events/20μm
10^3
10^2
10^1
10^0
−0.03
−0.02
−0.01
0
0.01
0.02
0.03
Dvx−Dvx(Φ) (cm)

Figure 6

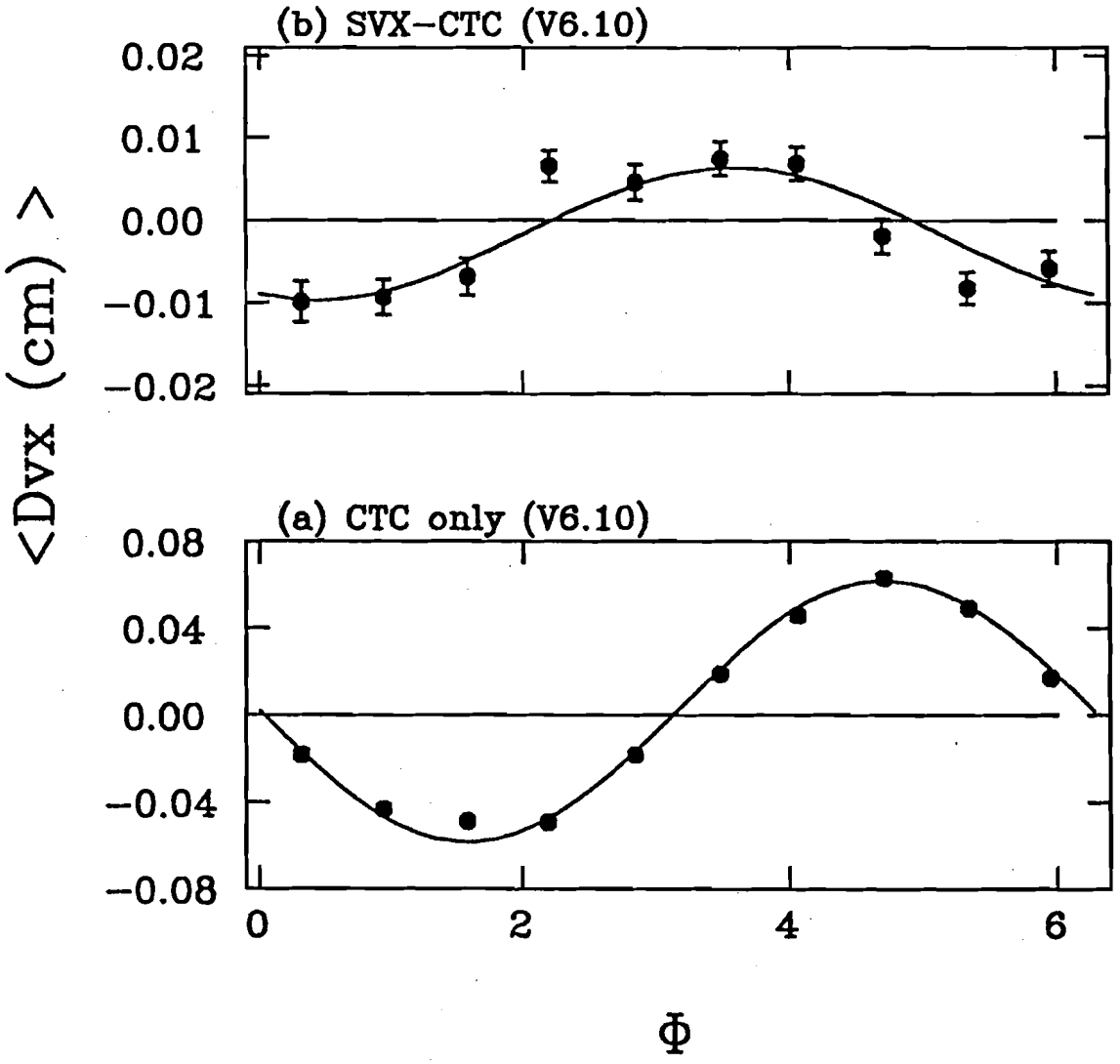
(b) SVX−CTC (V6.10)
0.02
0.01
0.00
−0.01
−0.02
<Dvx (cm) >
(a) CTC only (V6.10)
0.08
0.04
0.00
−0.04
−0.08
0
2
4
6
Φ

Figure 7

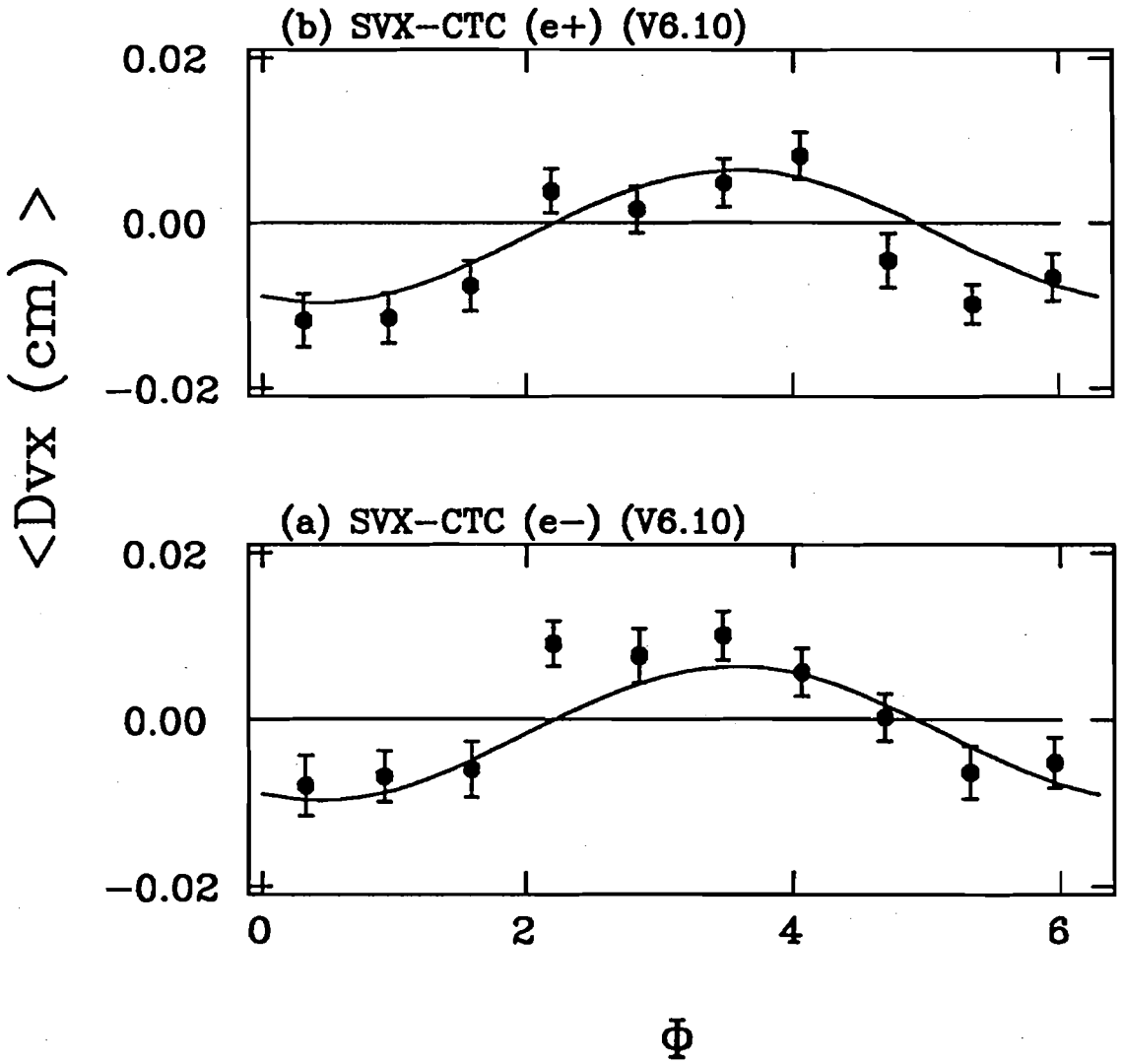
(b) SVX–CTC (e+) (V6.10)
(a) SVX–CTC (e–) (V6.10)
0.02
0.00
–0.02
0.02
0.00
–0.02
0
2
4
6
<Dvx (cm) >
Φ

Figure 8

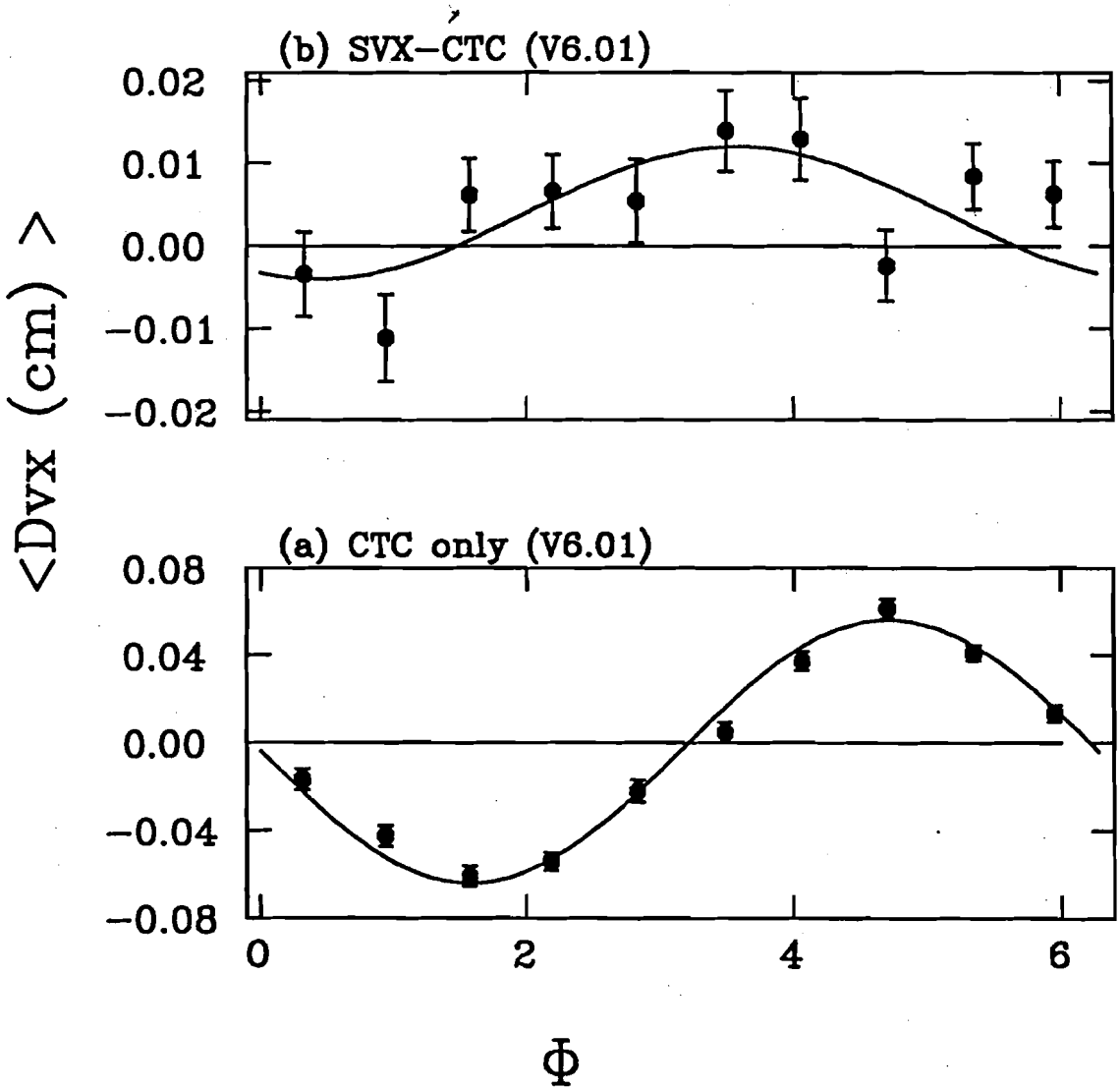
(b) SVX−CTC (V6.01)
0.02
0.01
0.00
−0.01
−0.02
<Dvx (cm) >
(a) CTC only (V6.01)
0.08
0.04
0.00
−0.04
−0.08
0
2
4
6
Φ

Figure 9

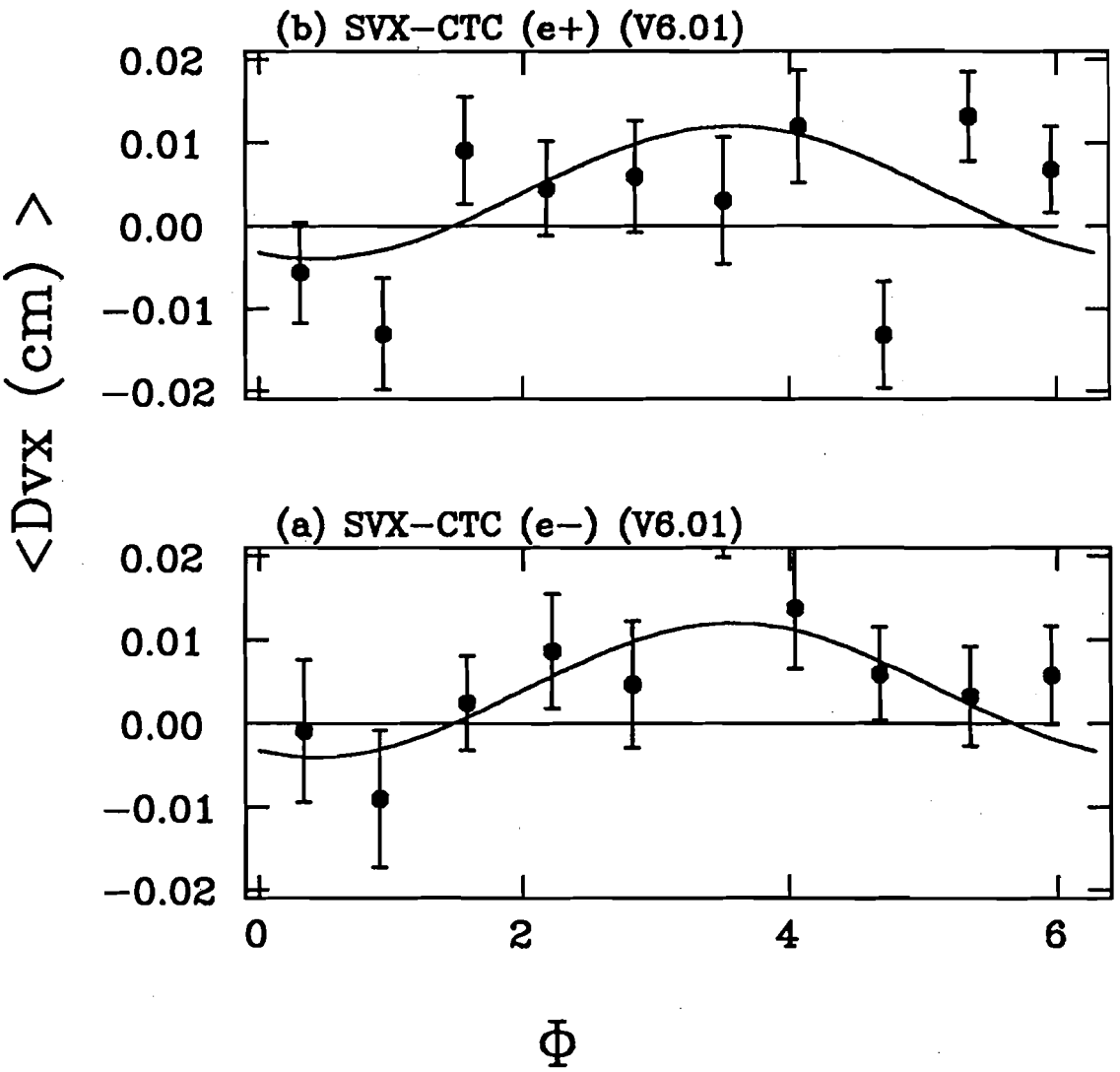

Figure 10

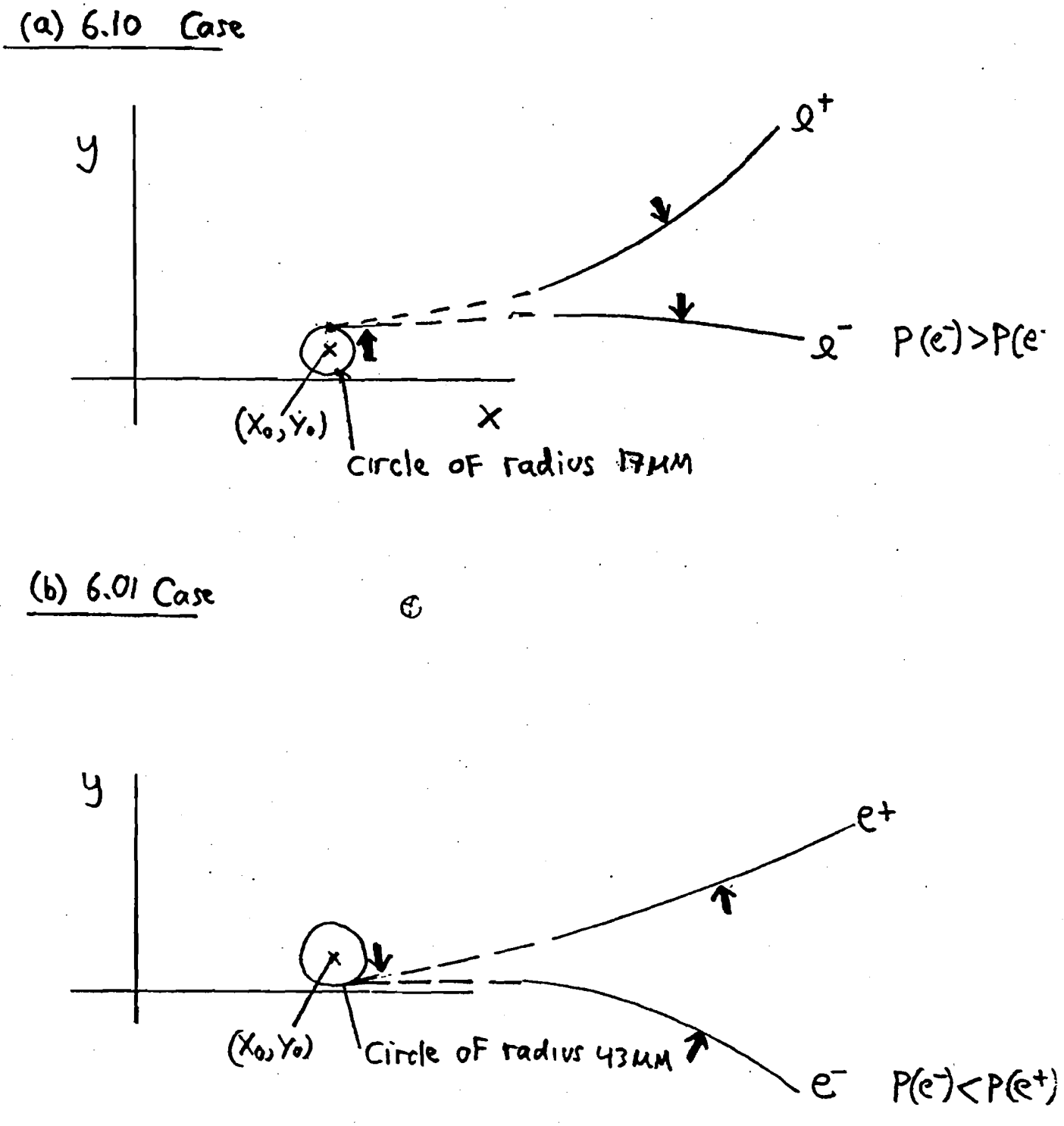

Figure 11

Schematic depiction of e^+,e^- trajectories measured in CTC. Heavy arrows indicate direction of distortions at (X0,Y0) and at Sagitta, due to CTC alignment errors.

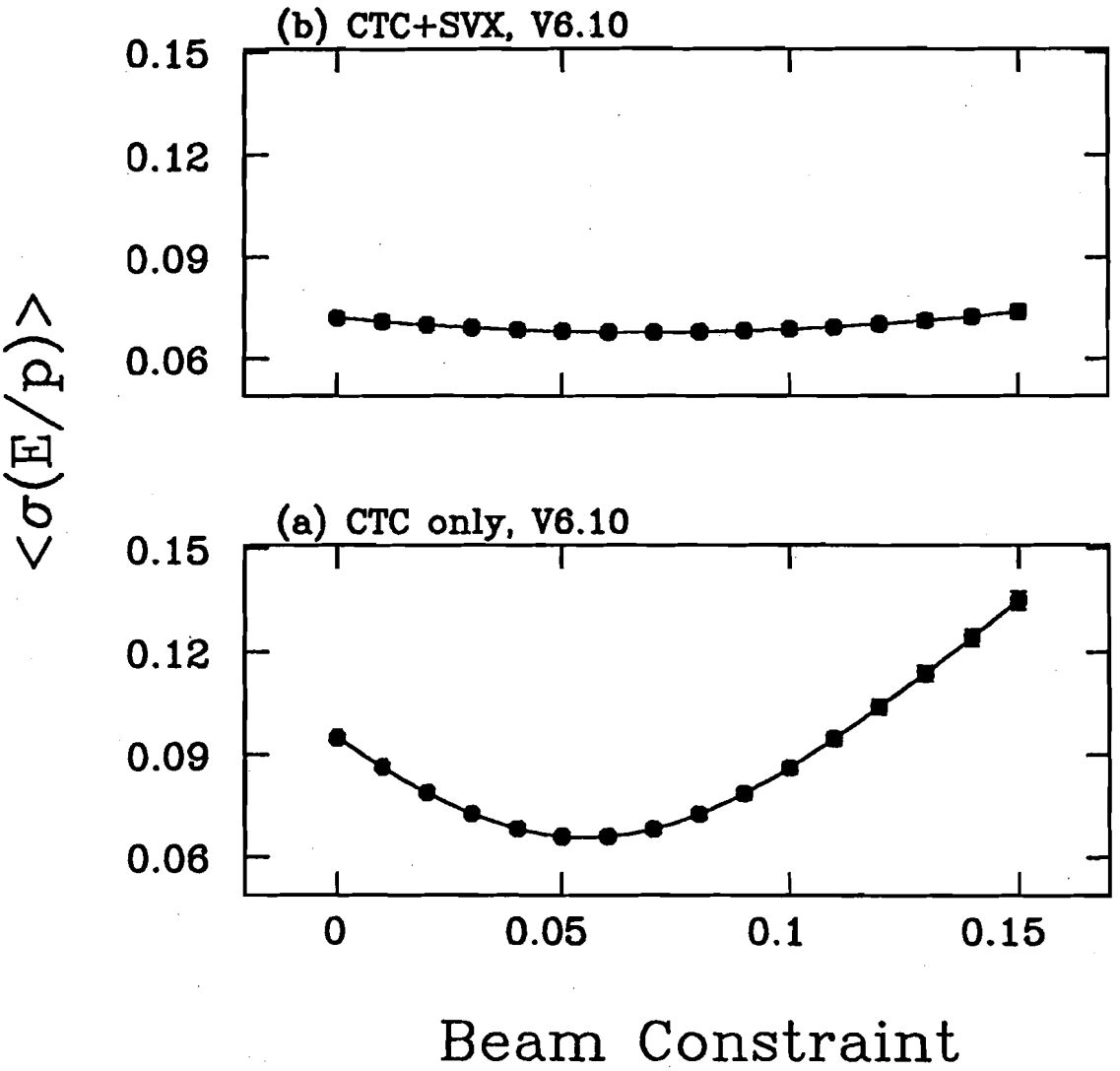
(b) CTC+SVX, V6.10
0.15
0.12
0.09
0.06
<σ(E/p)>
(a) CTC only, V6.10
0.15
0.12
0.09
0.06
0
0.05
0.1
0.15
Beam Constraint

Figure 12

$\delta\left(\frac{1}{p}\right) = K \times \delta(d\sigma)$

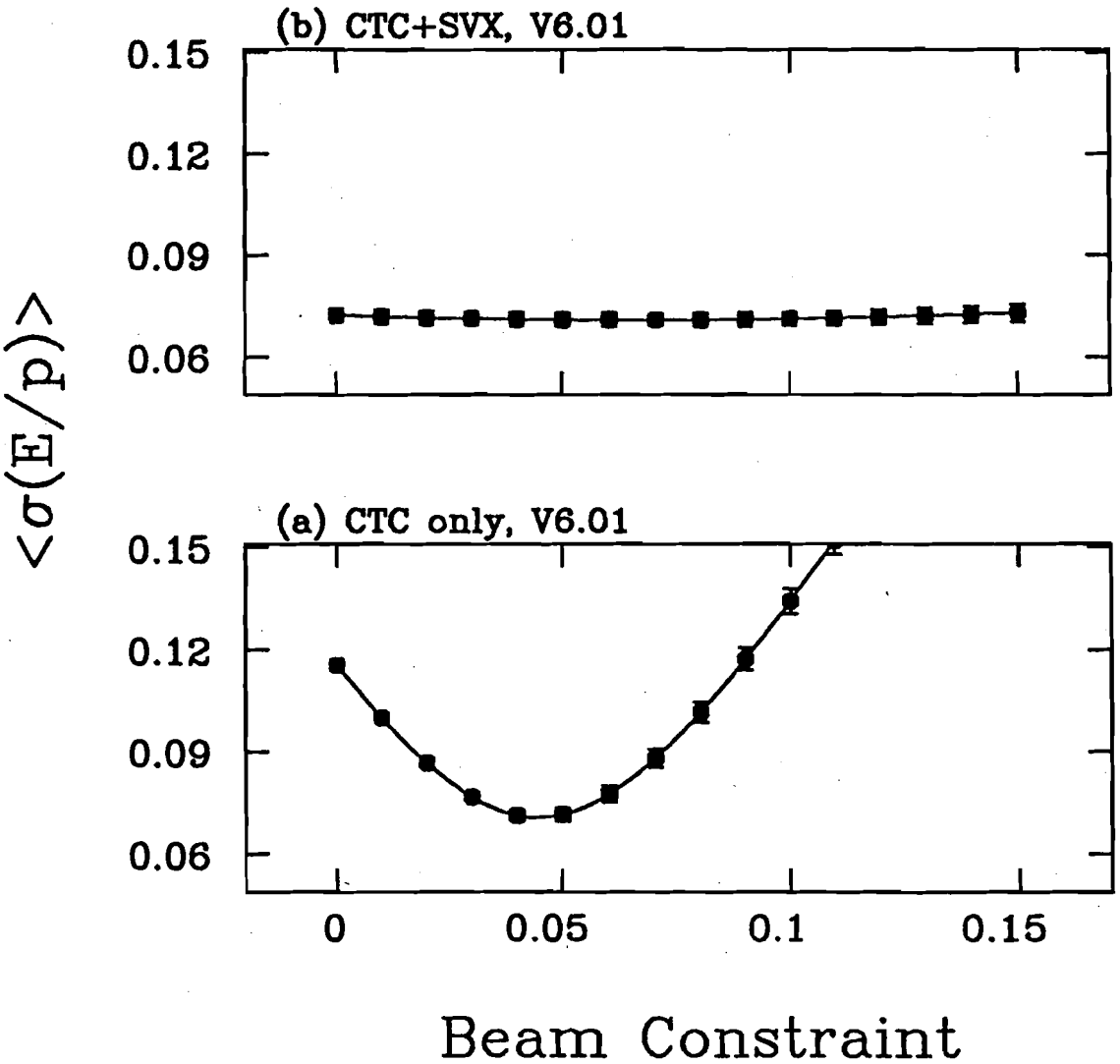

Figure 13

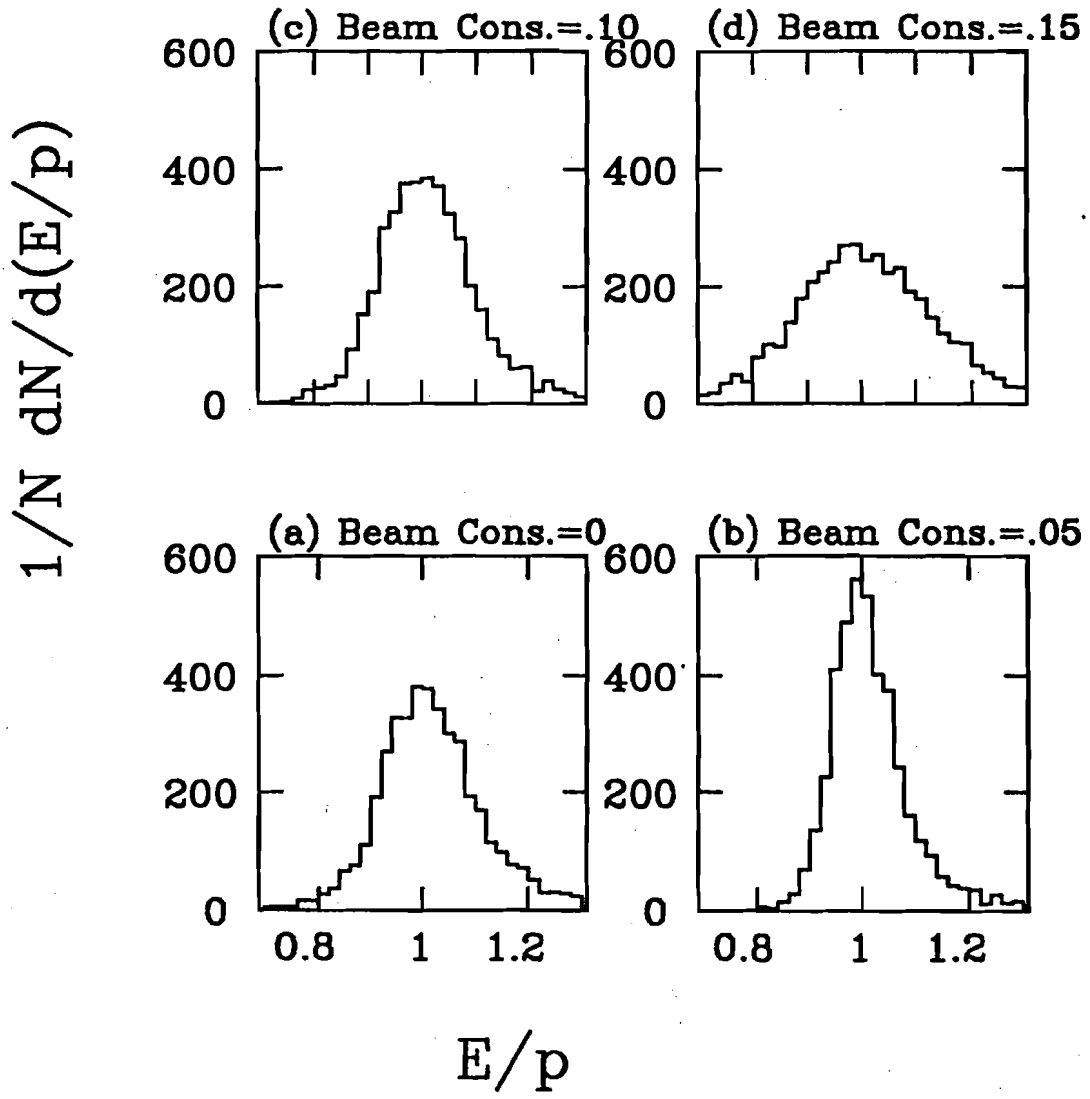
(c) Beam Cons.=.10
(d) Beam Cons.=.15
(a) Beam Cons.=0
(b) Beam Cons.=.05
600
400
200
0
0.8
1
1.2
1/N dN/d(E/p)
E/p

Figure 14

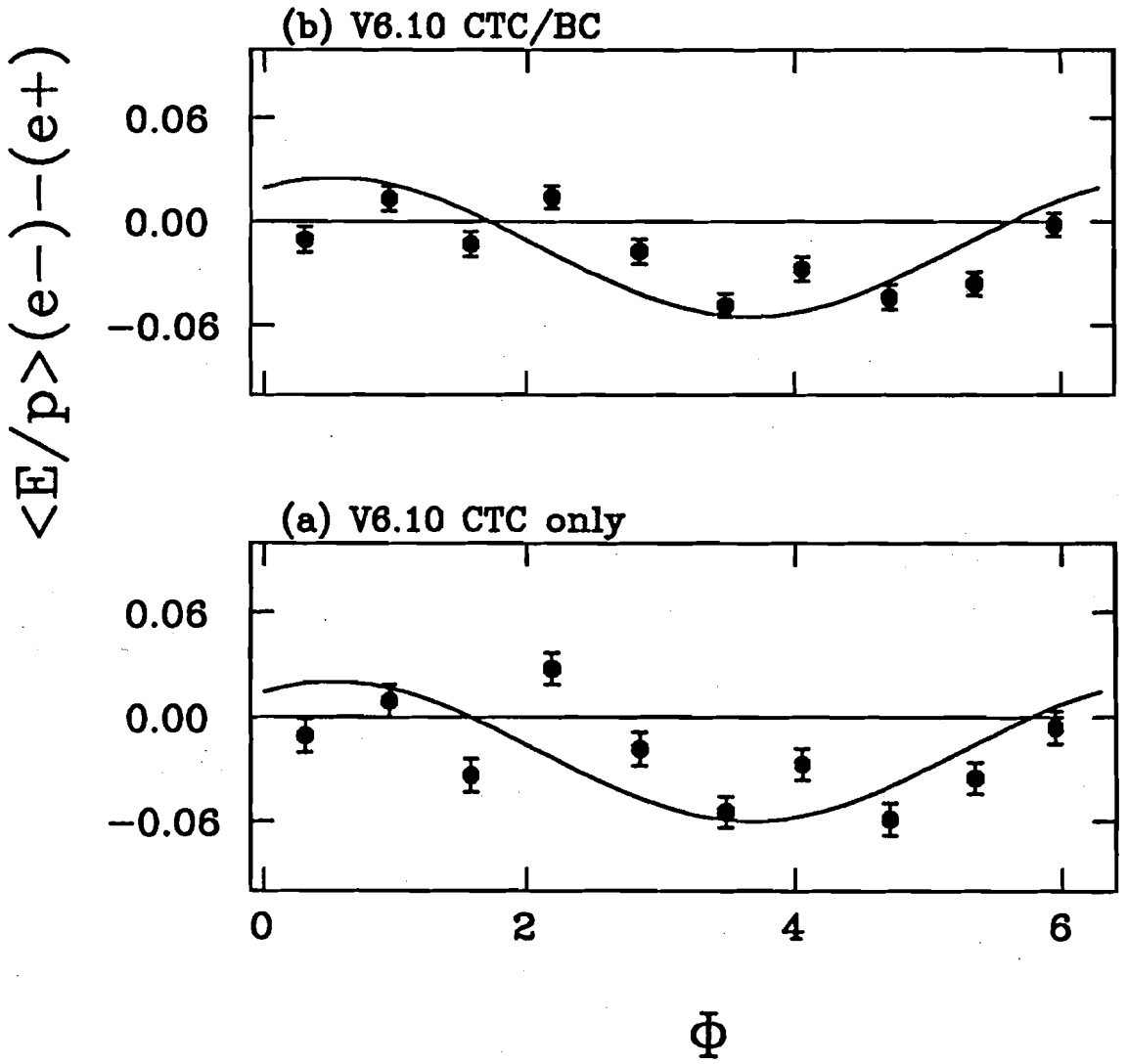

Figure 15a

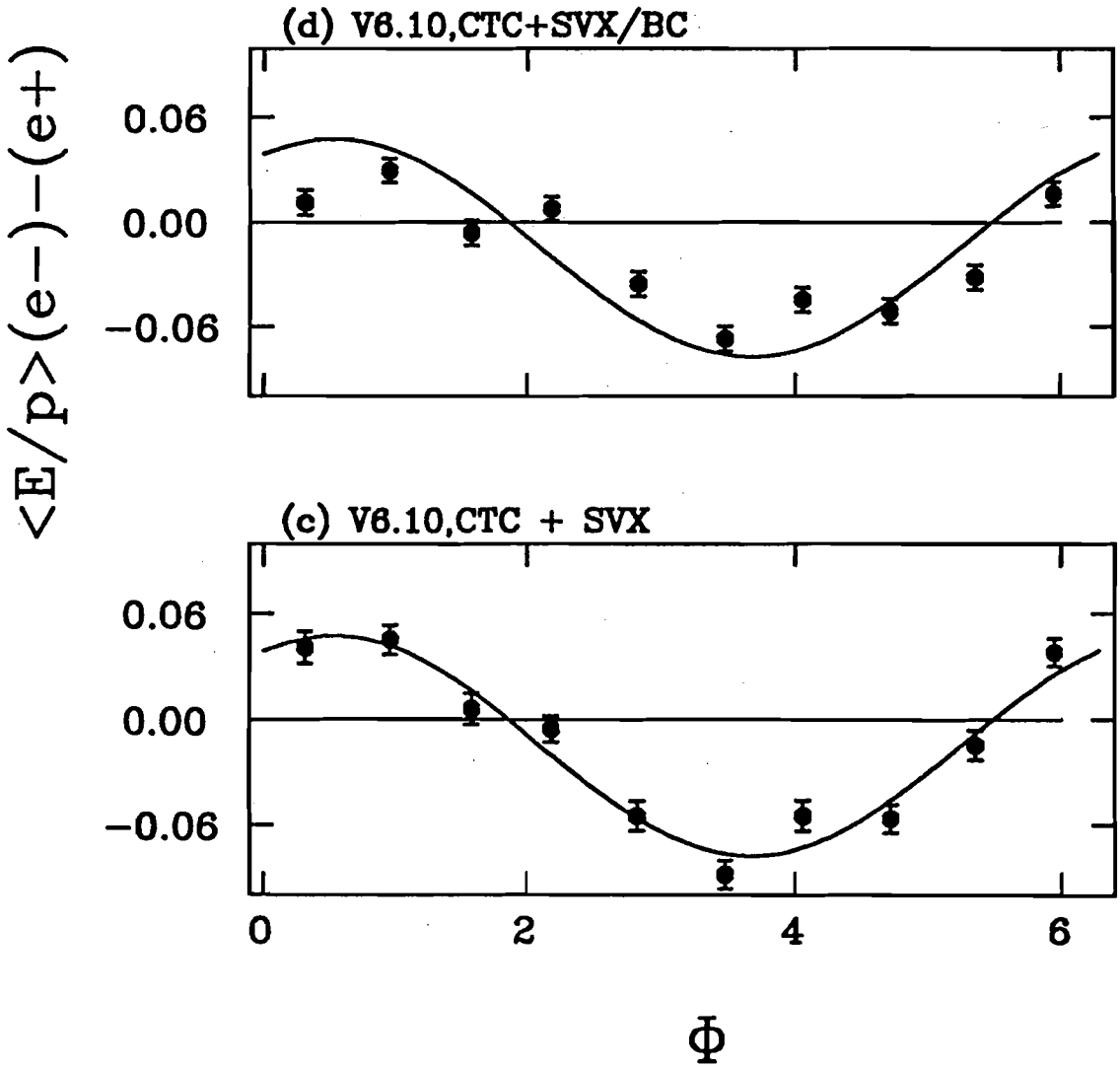

Figure 15b

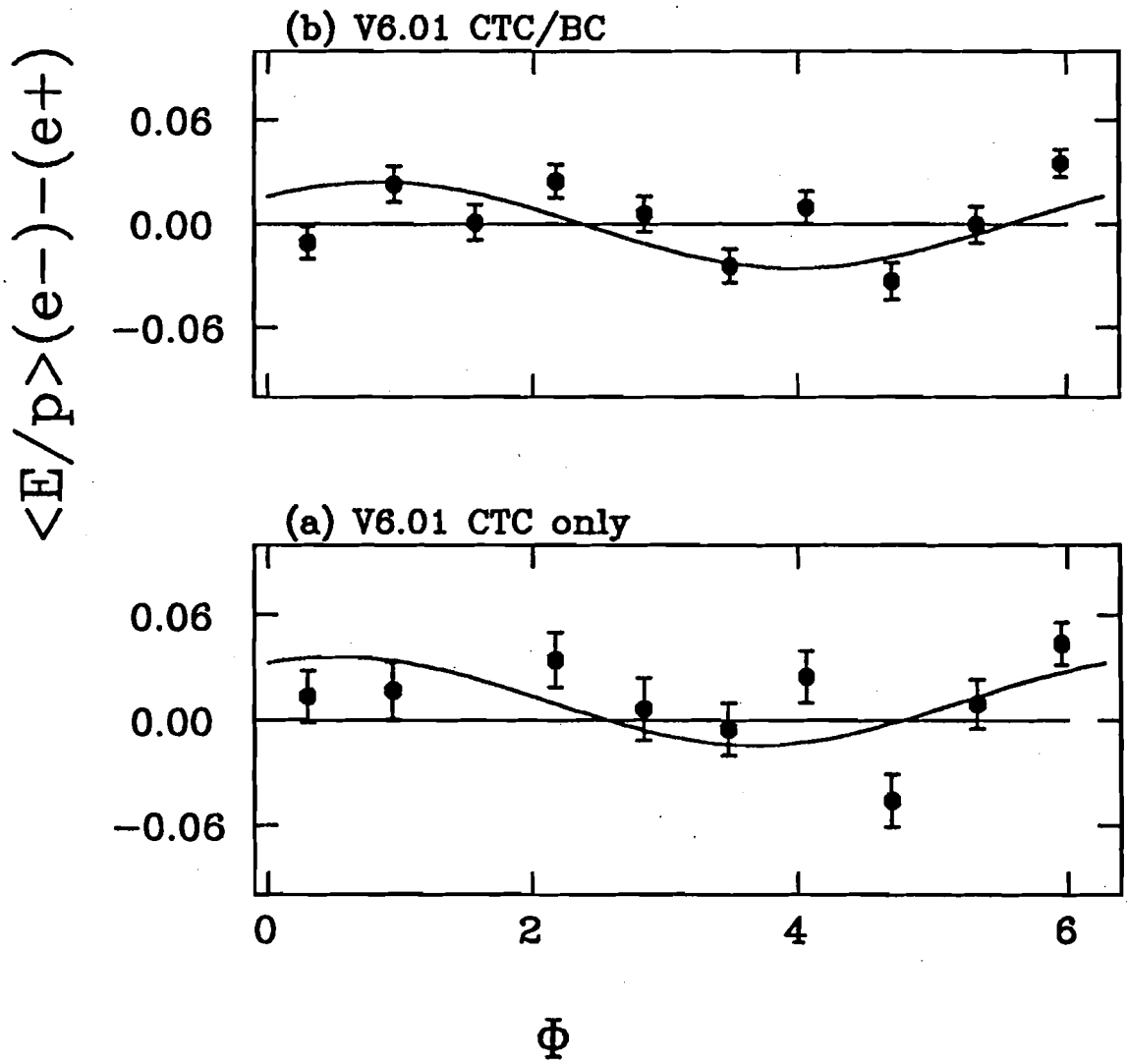

Figure 16a

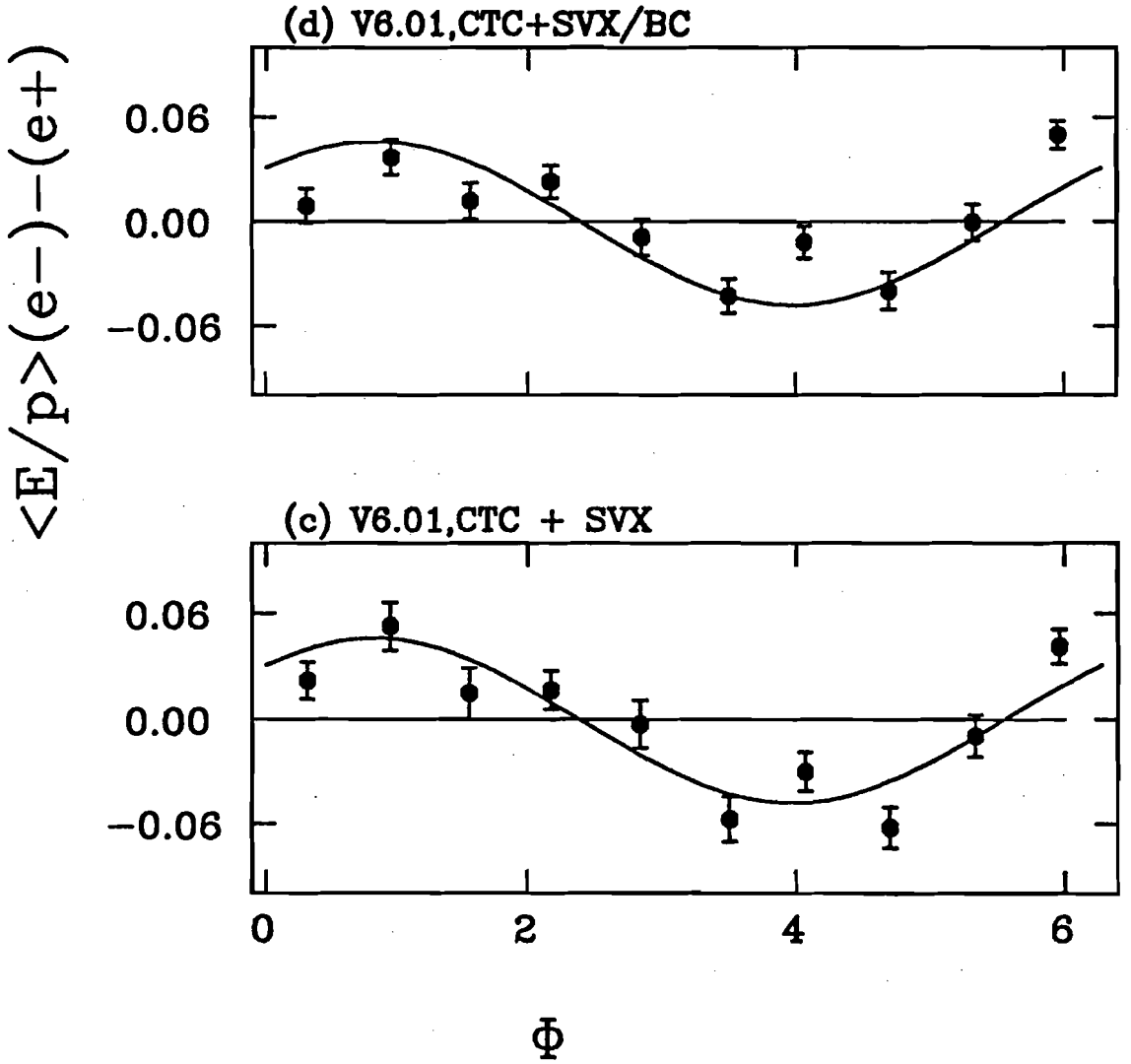

Figure 16b

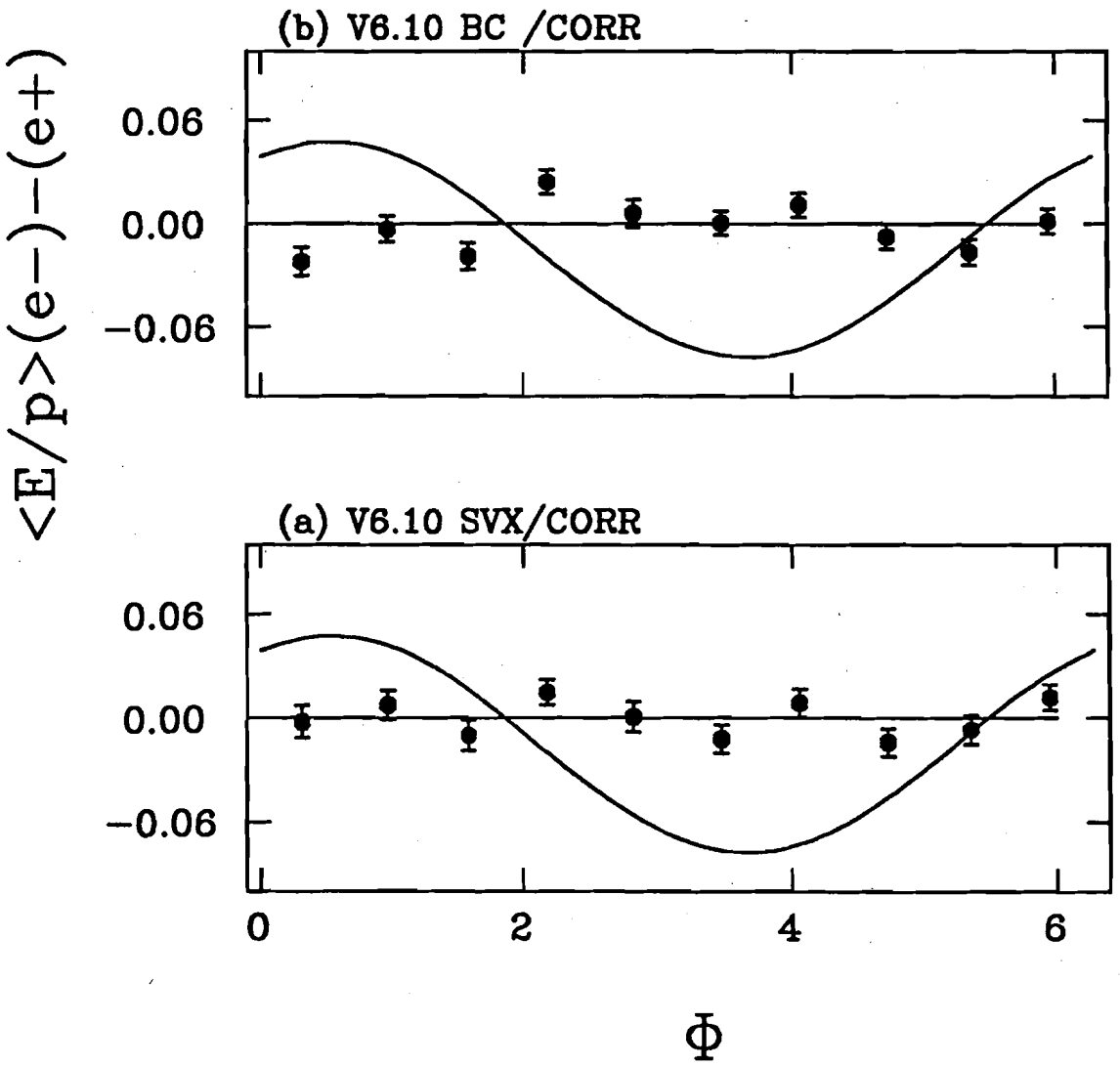

Figure 17

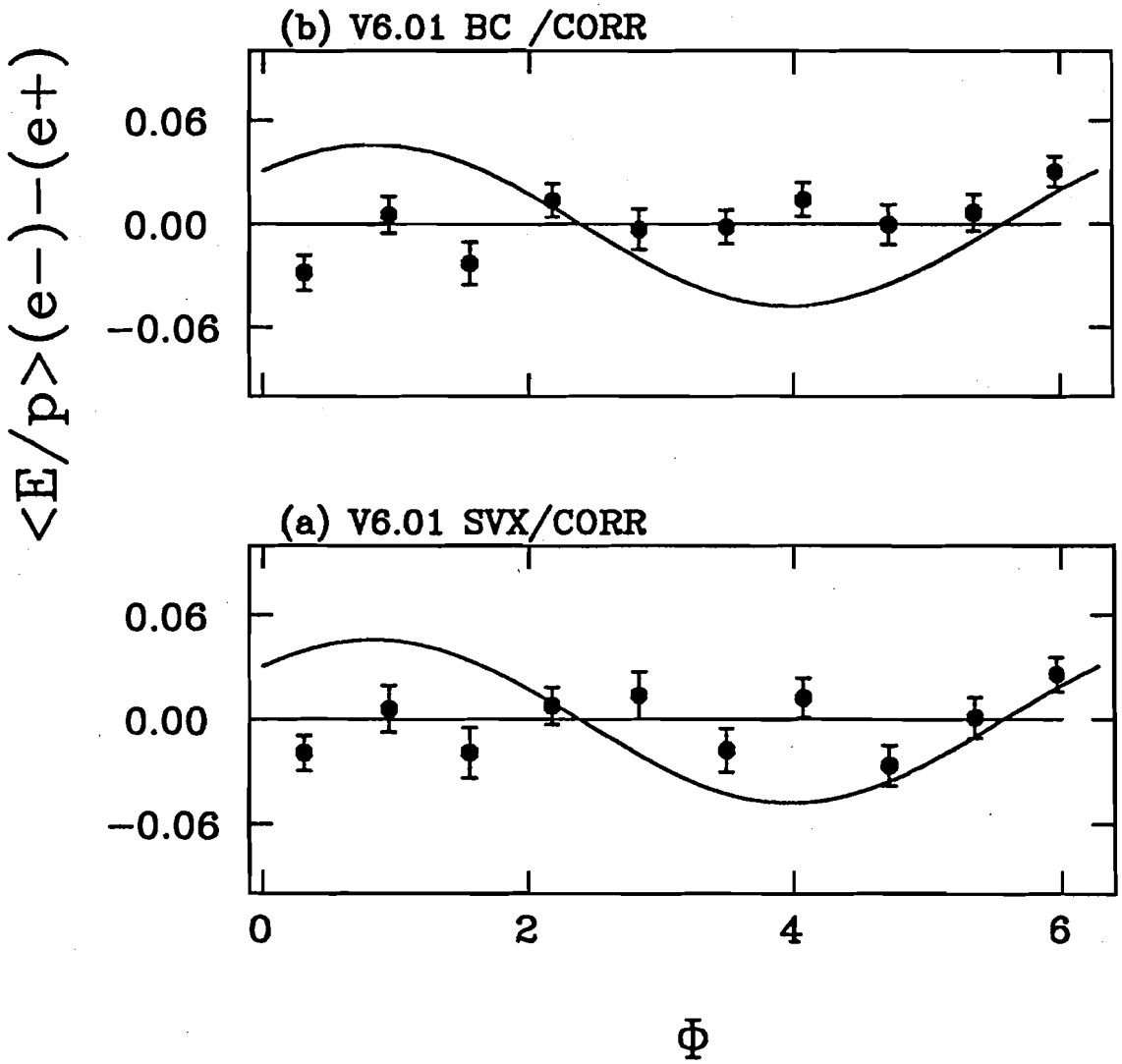

Figure 18

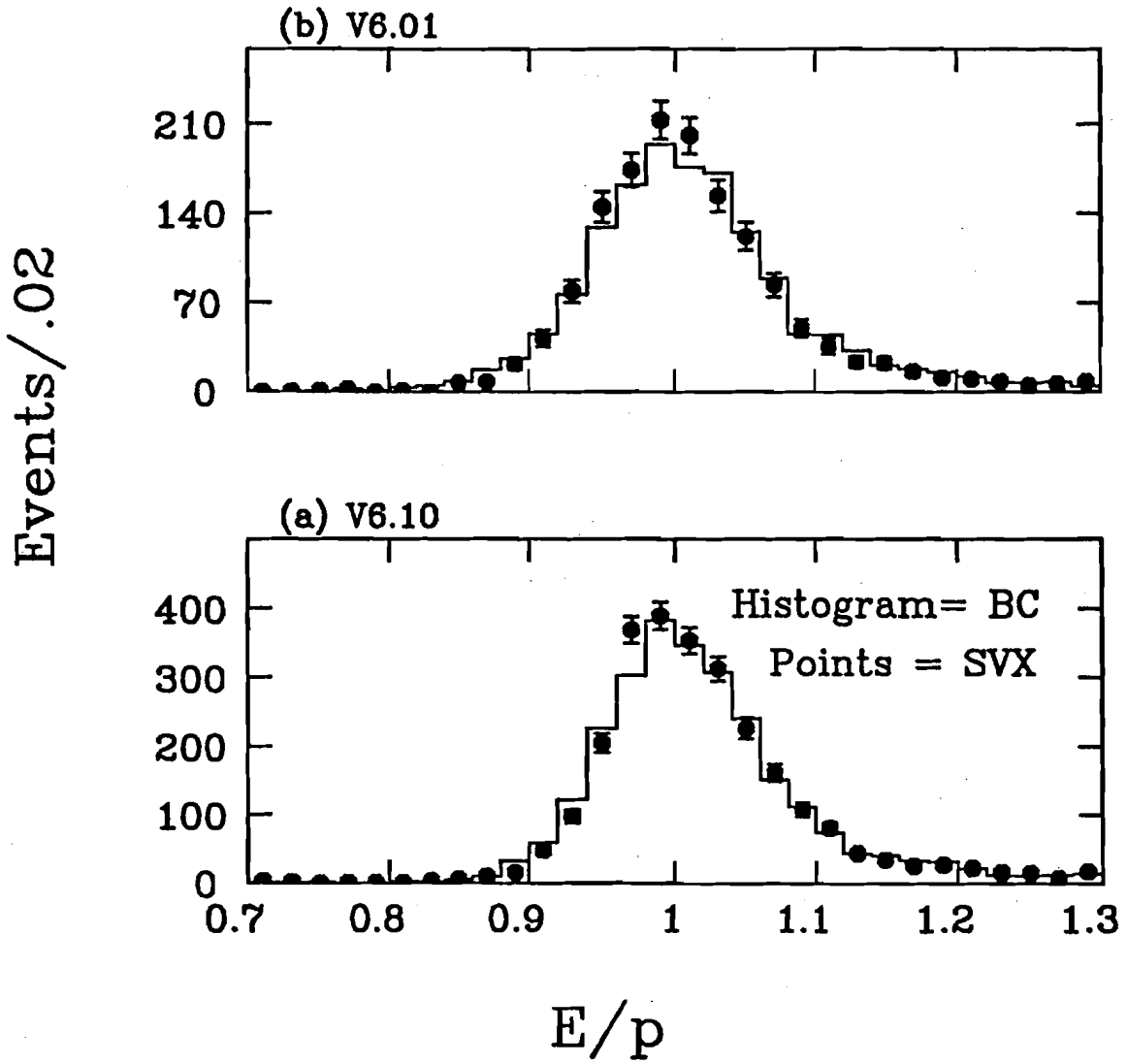
(b) V6.01
210
140
70
0
(a) V6.10
400
300
200
100
0
Histogram= BC
Points = SVX
0.7
0.8
0.9
1
1.1
1.2
1.3
Events/.02
E/p

Figure 19

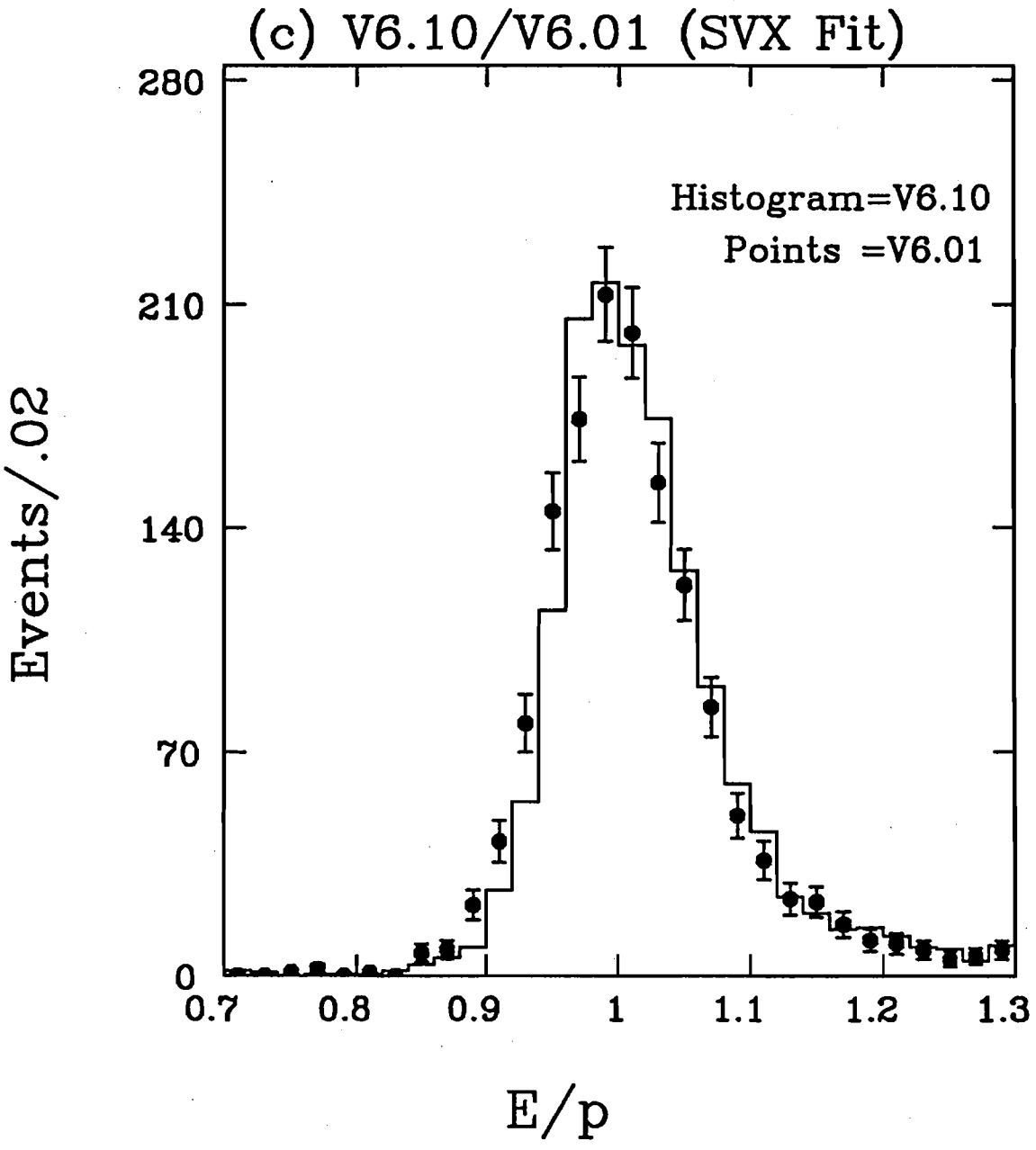
(c) V6.10/V6.01 (SVX Fit)
Histogram=V6.10
Points =V6.01
Events/.02
280
210
140
70
0
0.7
0.8
0.9
1
1.1
1.2
1.3
E/p

Figure 20

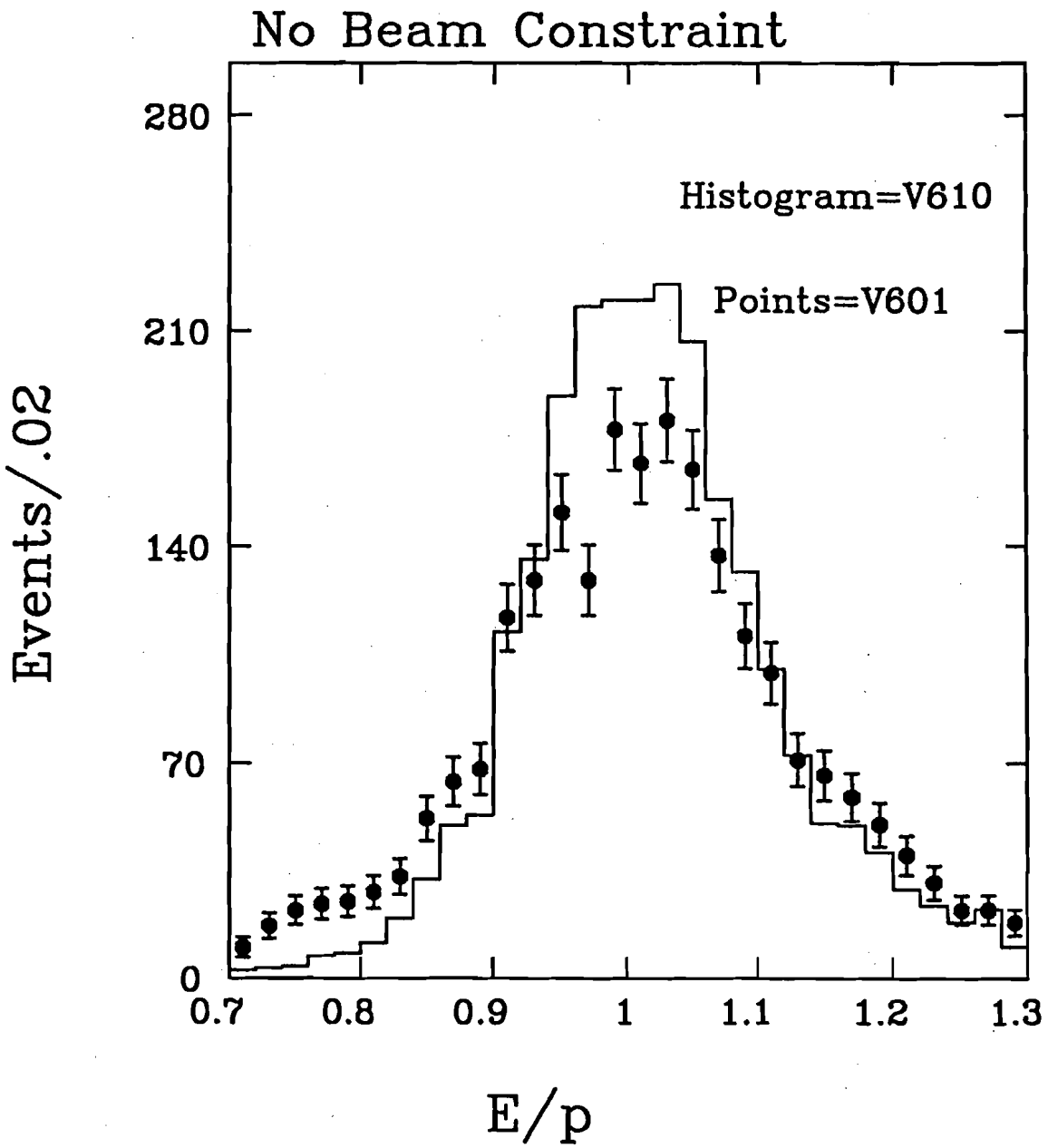
No Beam Constraint
Histogram=V610
Points=V601
Events/.02
280
210
140
70
0
0.7
0.8
0.9
1
1.1
1.2
1.3
E/p

Figure 21

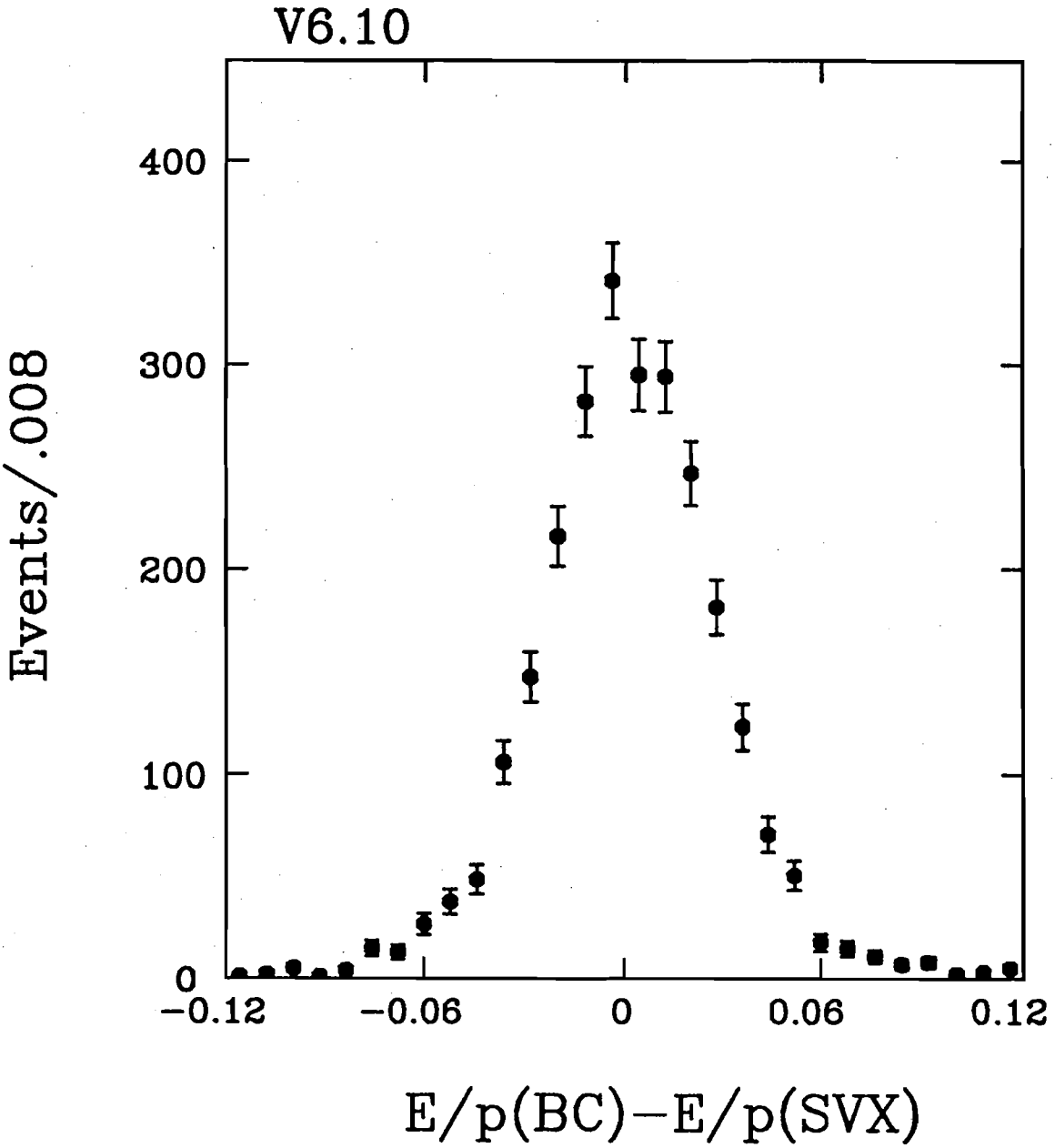

Figure 22

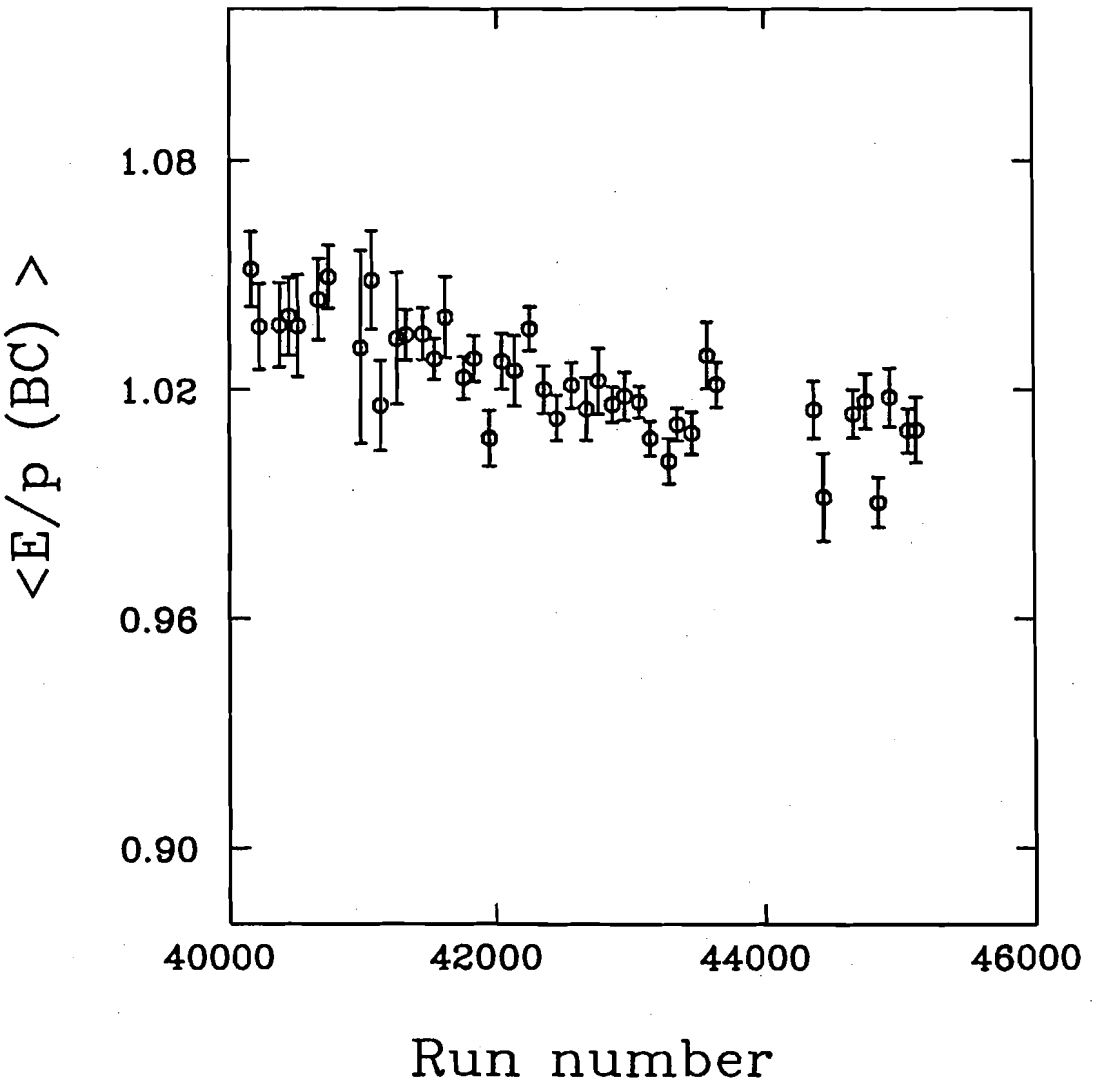

Figure 23

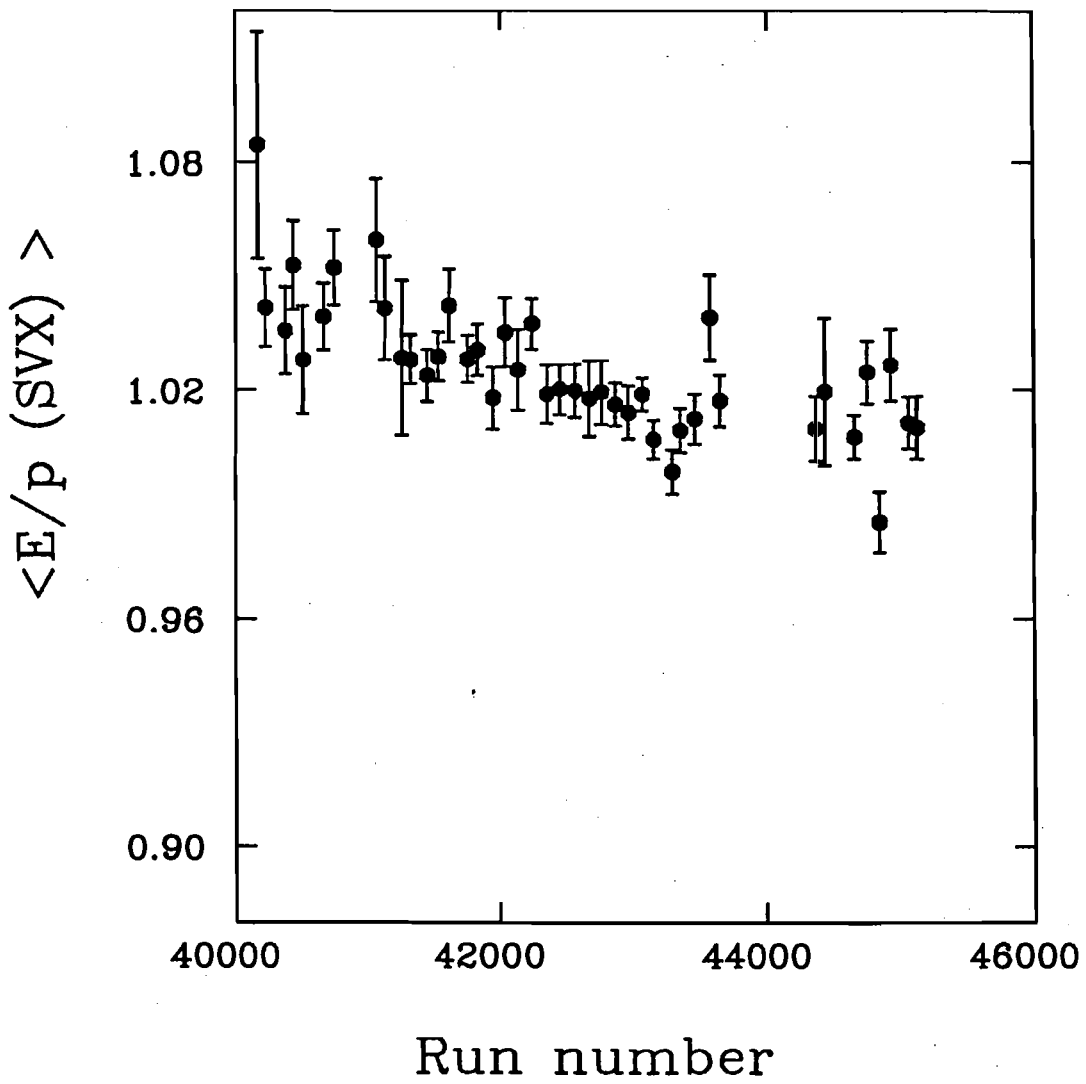

Figure 24

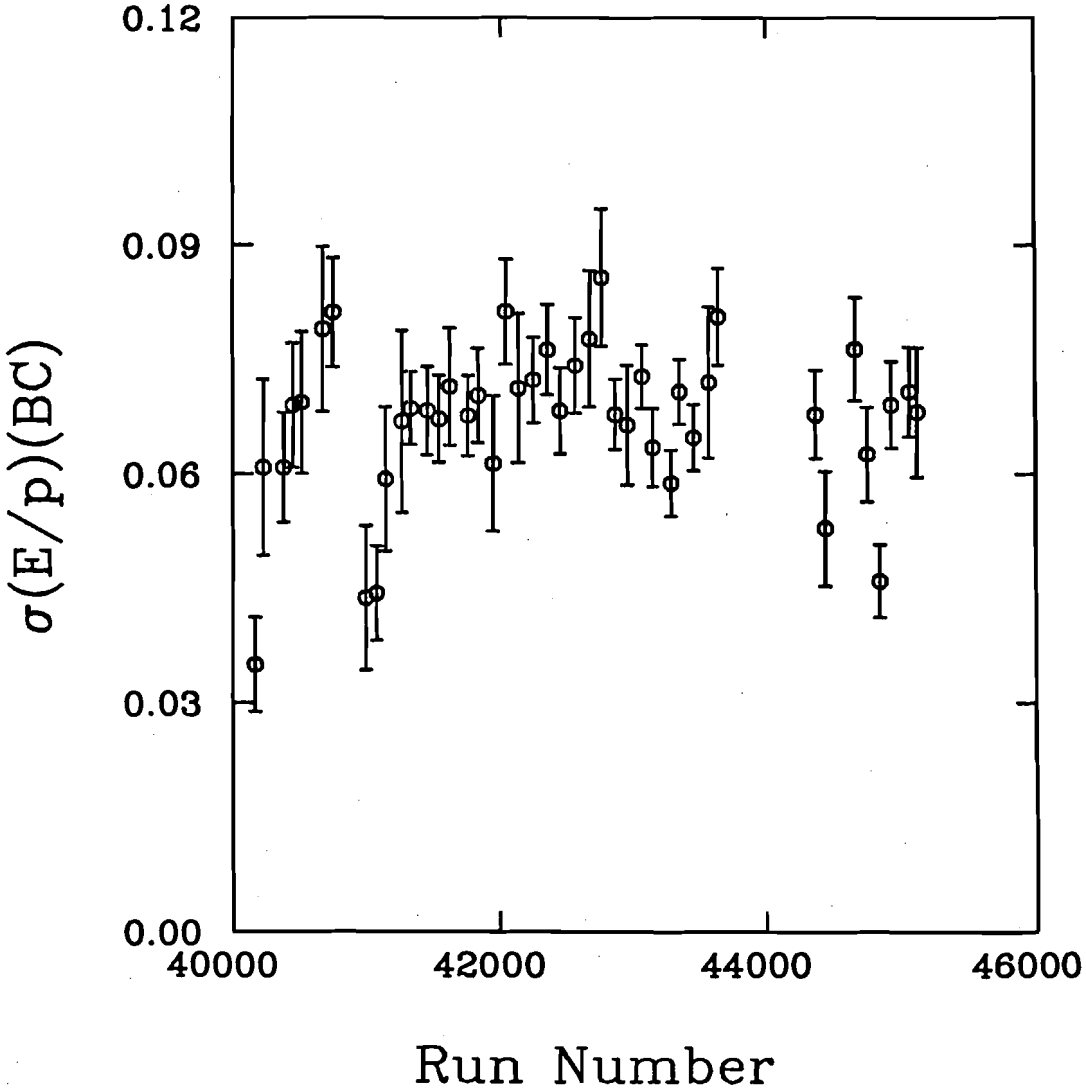

Figure 25

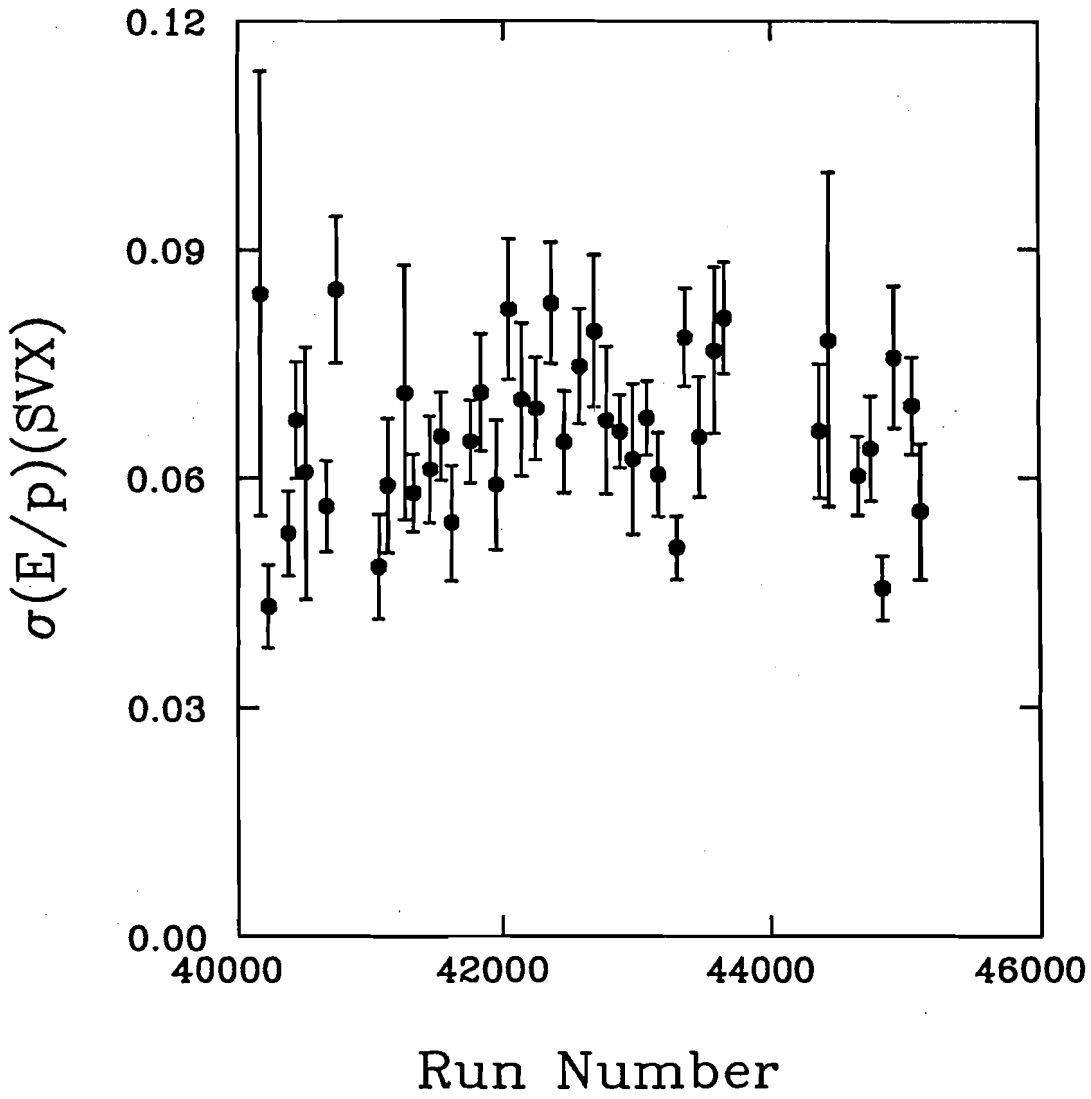
0.12
0.09
0.06
0.03
0.00
σ(E/p)(SVX)
40000
42000
44000
46000
Run Number

Figure 26